Supporting Information

Phenolic acetals from lignins of varying compositions *via* iron(III) triflate catalysed depolymerisation

Peter. J. Deuss,[a,b*] Christopher S. Lancefield,[c] A. Narani,[a] Johannes G. de Vries,[a,d] Nicholas J. Westwood,[c] Katalin Barta[a*]

[a] Stratingh Institute for Chemistry, University of Groningen, Nijenborgh 4, 9747 AG, Groningen, The Netherlands, E-mail: k.barta@rug.nl

[b] Department of Chemical Engineering (ENTEG), University of Groningen, Nijenborgh 4, 9747 AG, Groningen, the Netherlands

[c] School of Chemistry and, Biomedical Science Research Complex , University of St. Andrews and EaStCHEM, North Haugh, St. Andrews, Fife, KY16 9ST, United Kingdom, E-mail: njw3@st-andrews.ac.uk

[d] Leibniz-Insitut für Katalyse e.V. , Universität Rostock, Albert-Einstein-Straße 29a, 18059 Rostock, Germany, E-mail: johannes.devries@catalysis.de

1. General Remarks

1.1 Chemicals

Iron(III) triflate was purchased from Aldrich (90%) it was previously found that iron(III) triflate from other suppliers led to varying cleavage performance in model compounds.[1] Ethylene glycol (99+%) and 1,4-dioxane (99+%, extra pure, stabilized) were obtained from Acros. Other chemicals were obtained from Acros, Aldrich or Strem at the highest available purity unless stated otherwise.

1.2 Analysis equipment

Gas chromatography flame ionization detection:

GC-FID was performed using an Agilent 6890 series equipped with a 6890N FID using nitrogen as carrier gas. Standard settings: 1 µL injection, a split ration of 50:1, a nitrogen flow of 1 mL/s. The GC apparatus was equipped with a HP5 column (30 m x 0.25 mm x 0.25 µm) and run with a temperature profile starting with a 5 min 60 °C isotherm followed by a 10 °C/min ramp for 20 minutes to 260 °C and ramp of 20 °C/min to 320 °C a temperature that was held for 5 minutes. Retention times: **P1** 19.7 min, **P2** 20.9 min, **P3** 23.4 min.

Gas chromatography mass spectrometry:

GC-MS was Shimadzu GC-2010 plus system equipped with a GCMS QP2010 GC SE detector and helium or hydrogen as carrier gas. Standard settings: 2 µL injection, a split ration of 10:1, a constant helium flow of 1 mL/s was used with a linear velocity of 36.5 cm/sec and a purge flow of 3 mL/min. The GC apparatus was equipped with a HP5 column (30 m x 0.25 mm x 0.25 µm) and run with a temperature profile starting with a 5 min 60 °C isotherm followed by a 10 °C/min ramp for 20 minutes to 260 °C and ramp of 20 °C/min to 300 °C a temperature that was held for 5 minutes. Retention times: **P1** 15.7 min, **P2** 17.0 min, **P3** 19.5 min.

Nuclear magnetic resonance spectroscopy:

NMR-spectroscopy was performed on either an Agilent Technologies 400/54 Premium shielded spectrometer using the CRISIS2-gradient-sensitivity enhanced pulse program or on Bruker Avance or Avance III spectrometers operating at 500 MHz or 700 MHz equipped with CPP TCI, CPP BBO or BBO probes using either hsqcetgpsp.3 or hsqcetgpsp.2 bruker pulse programs and previously reported parameters.[2] In particular spectra where recorded between 47-137 ppm or 50-90 ppm in the carbon dimension and -1-11 ppm in the proton dimension.

Gel permeation chromatography:

GPC was performed on a Hewlett Packard 1100 system equipped with three PL-gel 3 lm MIXED-E columns in series as THF as a solvent. The columns were operated at 42 °C with a flow-rate of 1 mL/min. Detection was accomplished at 35 °C using a GBC LC 1240 RI detector. The molecular weight was determined using polystyrene standards of known molecular weight distribution.

2. GPC analysis of isolated and externally obtained lignins

Lignins were analysed by GPC (THF) against polystyrene standards. The obtained graph for lignins that were (partially) soluble in THF are shown in Figure S1-S25 and the calculated M_n, M_w and Đ values are summarised Table S2. No GPC data was obtained for **L5** and **L25** and **L27** were insoluble in THF and comparable GPC graph could be obtained.

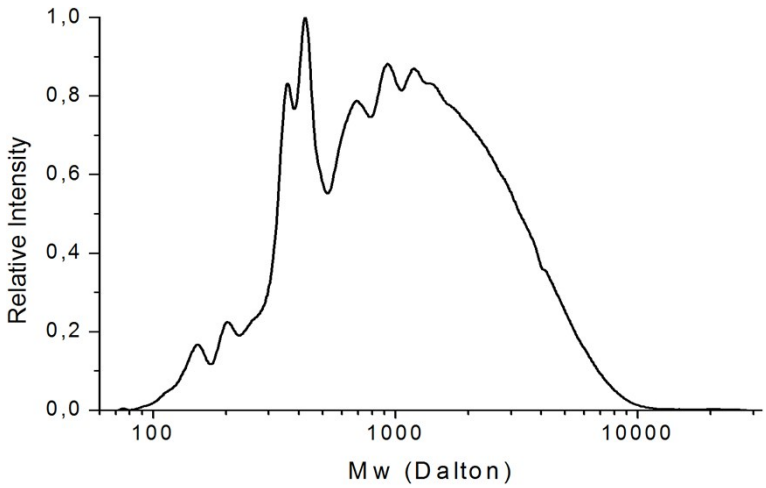

Figure S1. GPC (THF, against polystyrene standards) of unfractionated methansolv walnut lignin obtained by procedure 1 (**L1**).

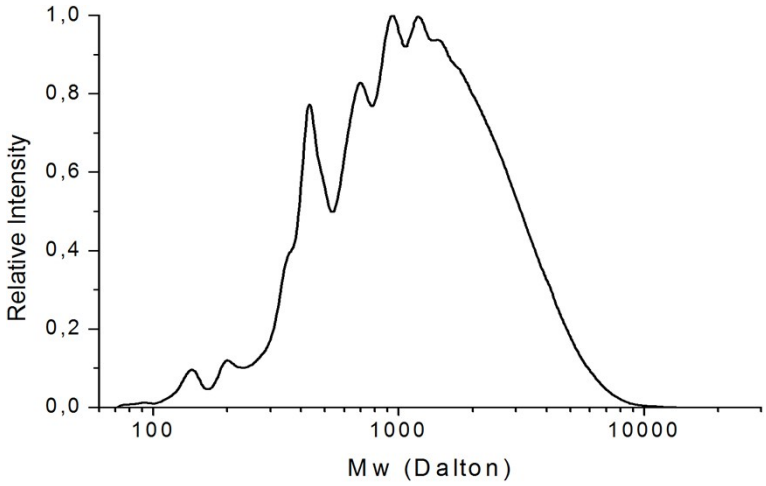

Figure S2. GPC (THF, against polystyrene standards) of the DCM soluble fraction of methansolv walnut lignin obtained by procedure 1 (**L2**).

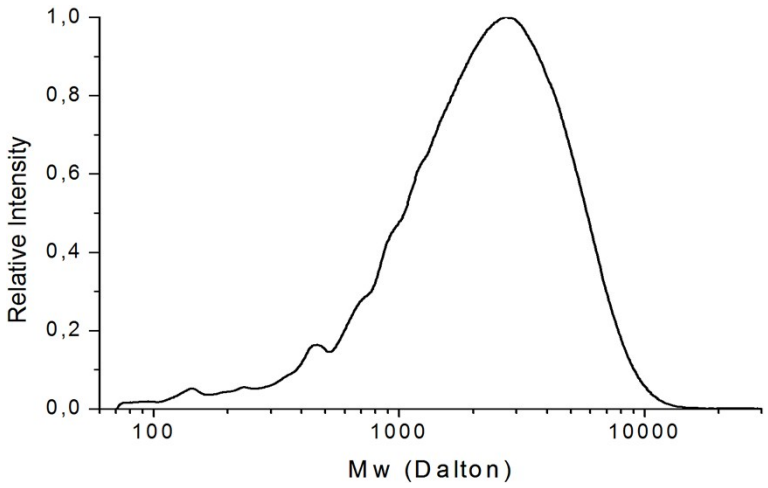

Figure S3. GPC (THF, against polystyrene standards) of the DCM insoluble fraction of methansolv walnut lignin obtained by procedure 1 (**L3**).

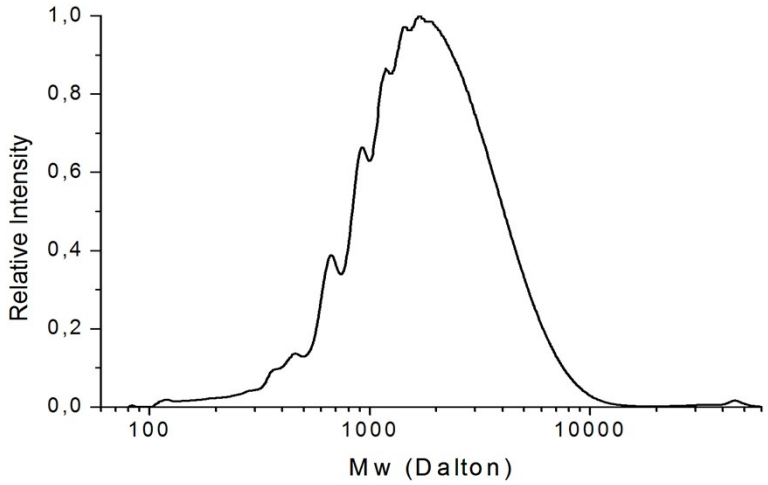

Figure S4. GPC (THF, against polystyrene standards) of methansolv walnut lignin obtained by procedure 2 (**L4**).

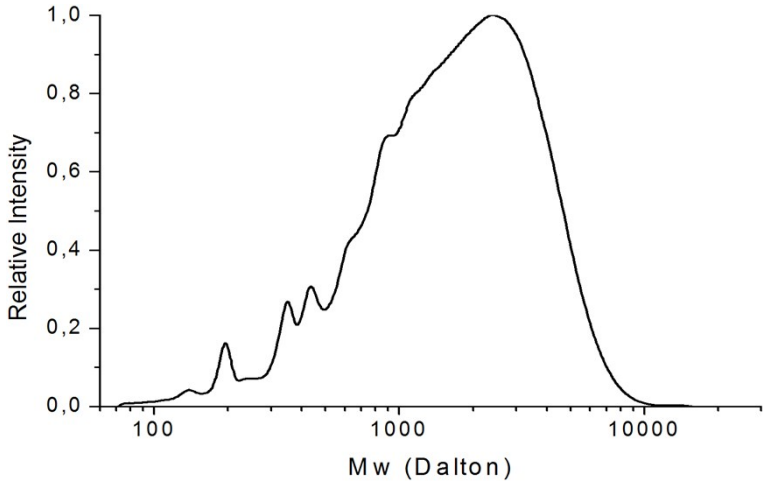

Figure S5. GPC (THF, against polystyrene standards) of methansolv pine lignin obtained by procedure 1 (Batch 2, **L6**).

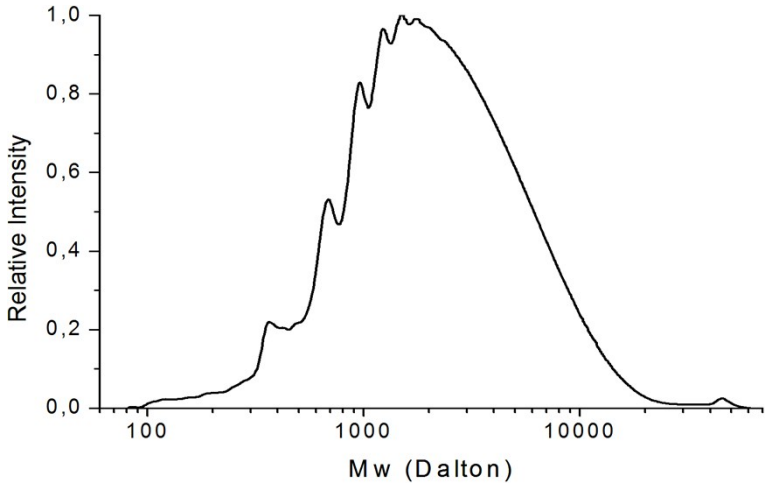

Figure S6. GPC (THF, against polystyrene standards) of ethansolv walnut lignin (**L7**).

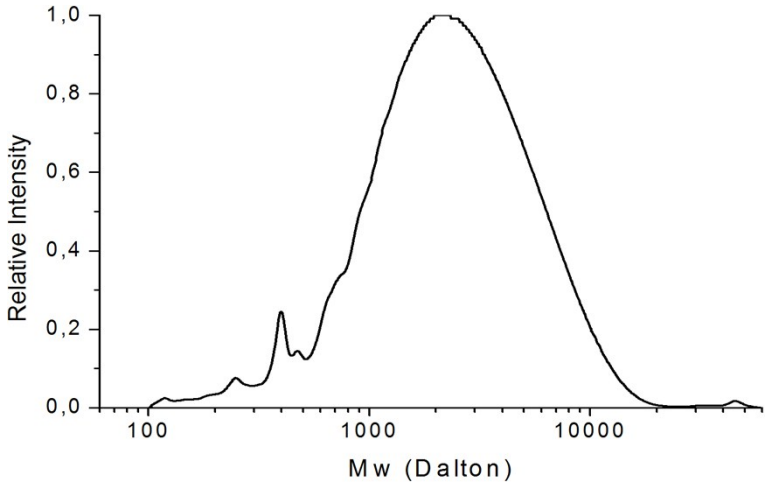

Figure S7. GPC (THF, against polystyrene standards) of ethansolv douglas fir lignin (**L8**).

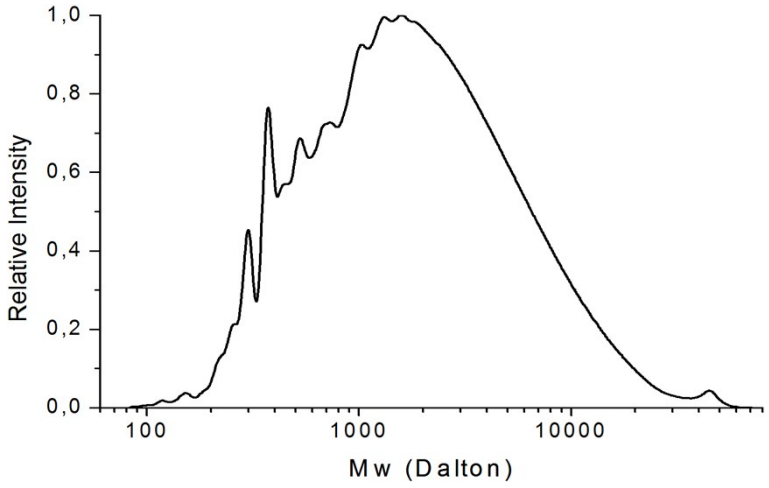

Figure S8. GPC (THF, against polystyrene standards) of butansolv walnut lignin (**L9**).

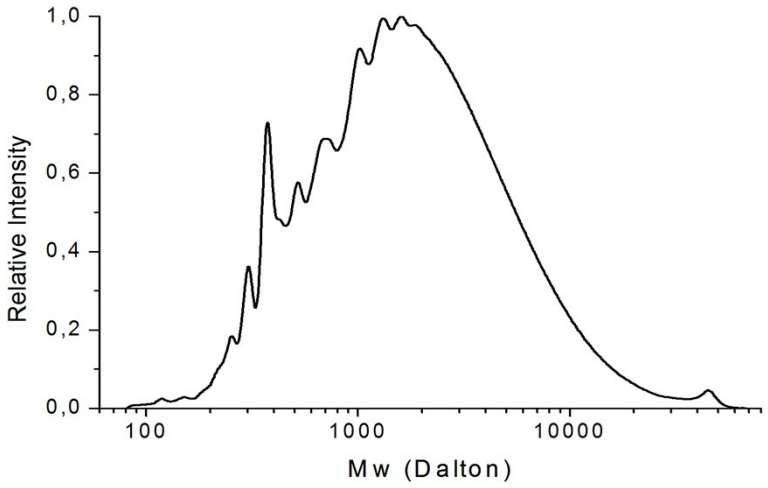

Figure S9. GPC (THF, against polystyrene standards) of butansolv beech lignin (**L10**).

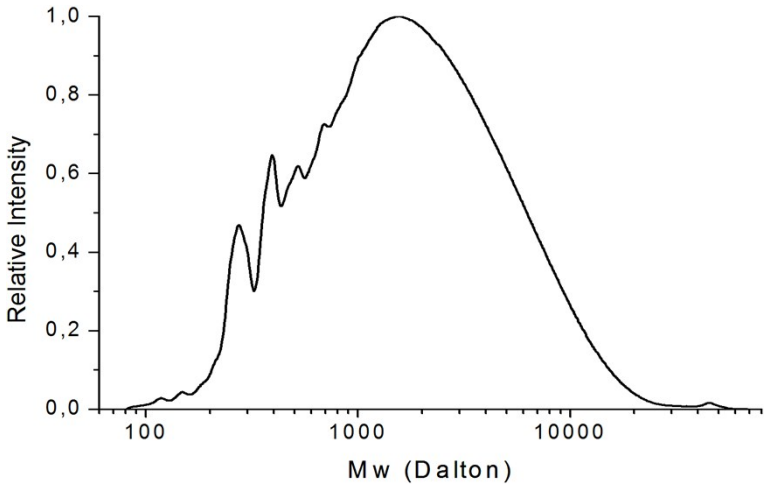

Figure S10. GPC (THF, against polystyrene standards) of butansolv douglas fir lignin (**L11**).

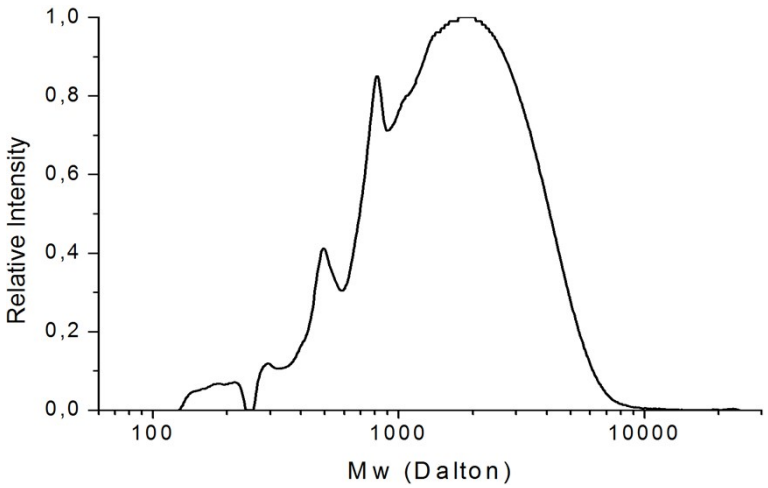

Figure S11. GPC (THF, against polystyrene standards) of dioxosolv walnut lignin obtained by procedure 1 (**P12**).

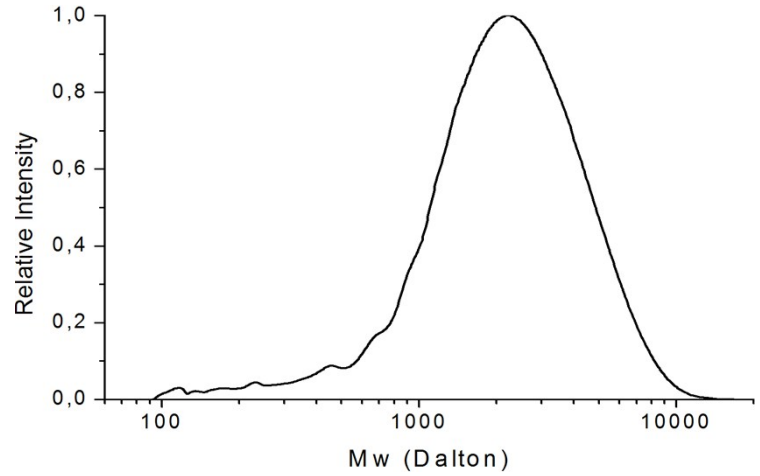

Figure S12. GPC (THF, against polystyrene standards) of dioxosolv pine lignin obtained by procedure 2 (Batch 1, **L13**).

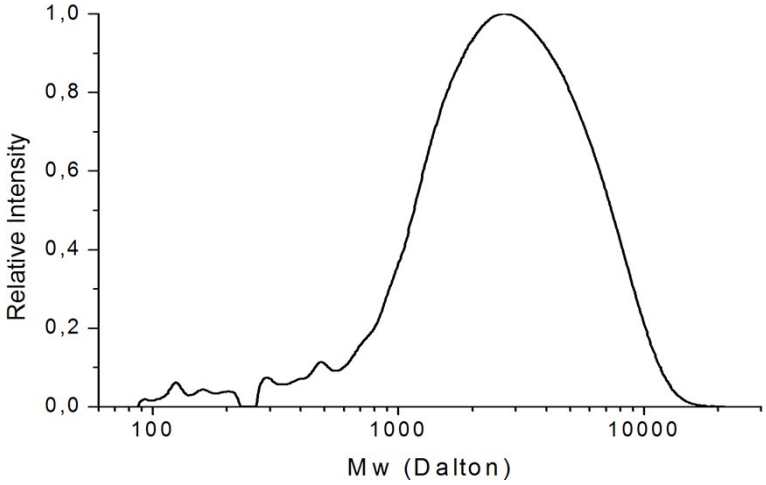

Figure S13. GPC (THF, against polystyrene standards) of dioxosolv pine lignin obtained by procedure 2 (Batch 2, **L14**).

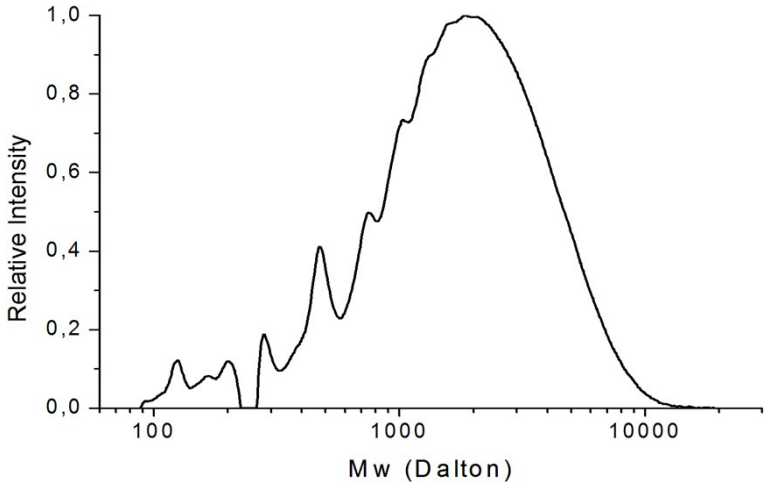

Figure S14. GPC (THF, against polystyrene standards) of dioxosolv oak lignin obtained by procedure 2 (**L15**).

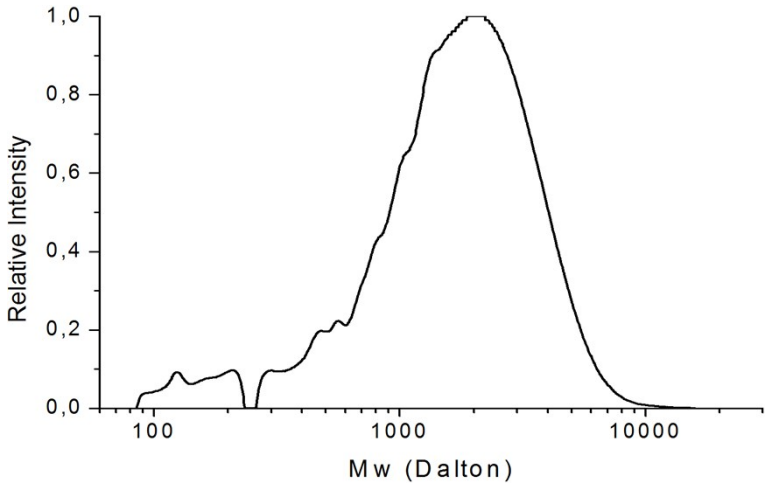

Figure S15. GPC (THF, against polystyrene standards) of dioxosolv barley straw lignin obtained by procedure 2 (**L16**).

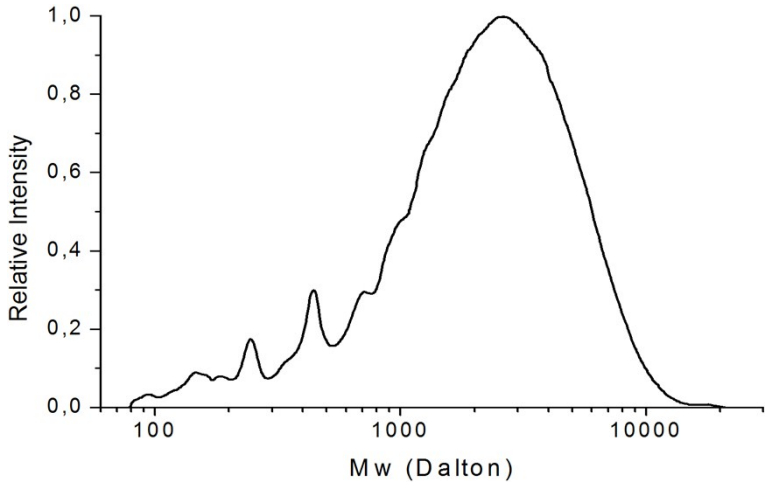

Figure S16. GPC (THF, against polystyrene standards) of dioxosolv birch lignin obtained by procedure 2 (**L17**).

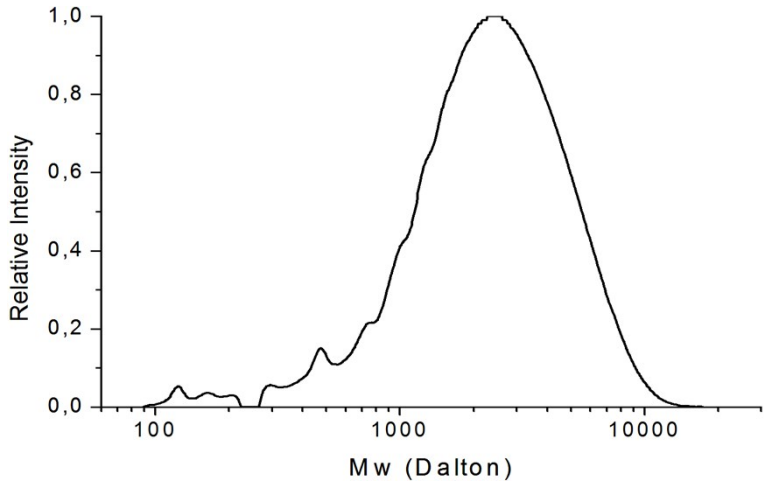

Figure S17. GPC (THF, against polystyrene standards) of CIVM oak lignin (**L18**).

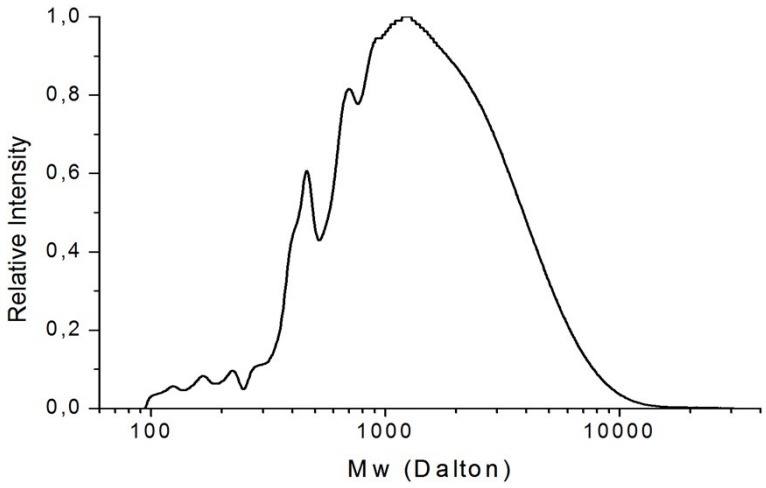

Figure S18. GPC (THF, against polystyrene standards) of technical ethanosolv beech lignin (ECN, **L19**).

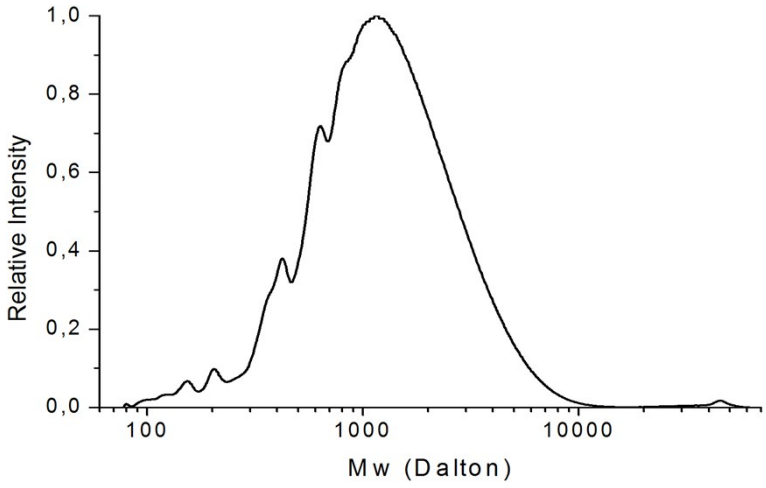

Figure S19. GPC (THF, against polystyrene standards) of technical ethanosolv poplar lignin (ECN, **L20**).

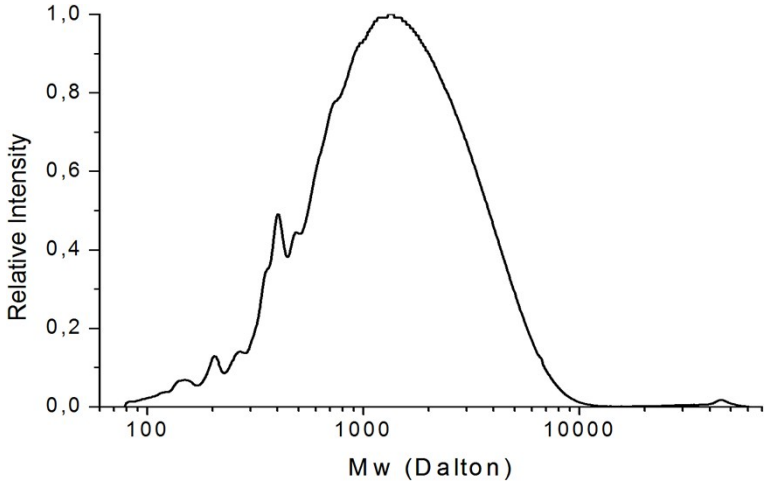

Figure S20. GPC (THF, against polystyrene standards) of technical ethanosolv spruce lignin (ECN, **L21**).

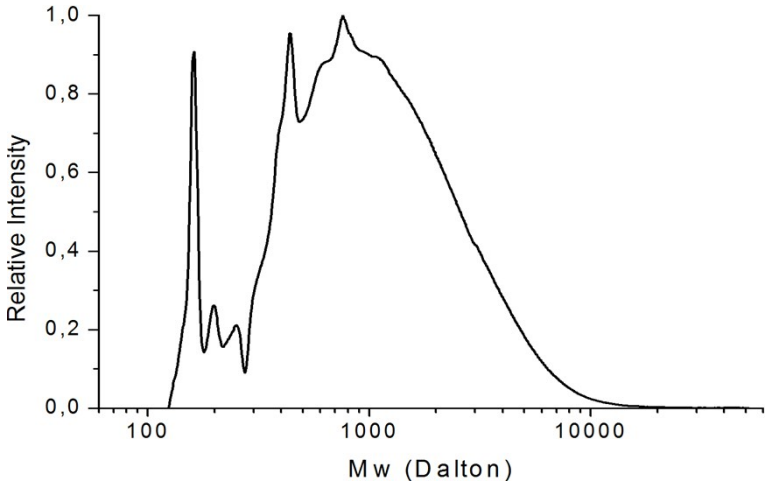

Figure S21. GPC (THF, against polystyrene standards) of Alcell lignin (ethanosolv, **L22**).

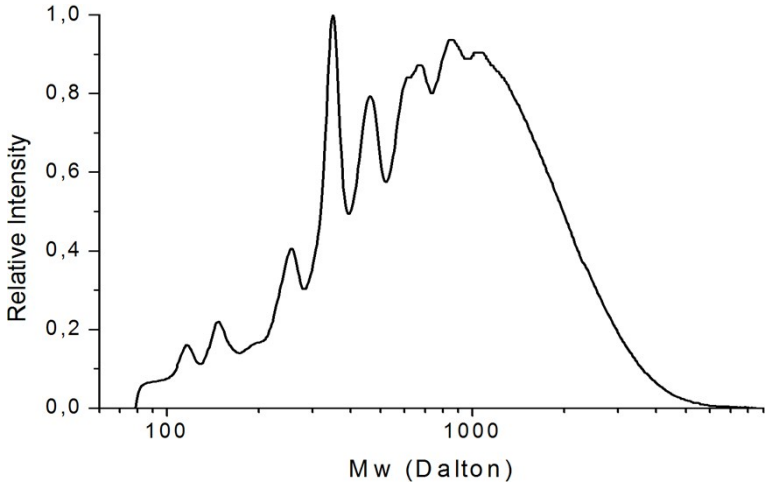

Figure S22. GPC (THF, against polystyrene standards) of Indulin-AT (**L23**).

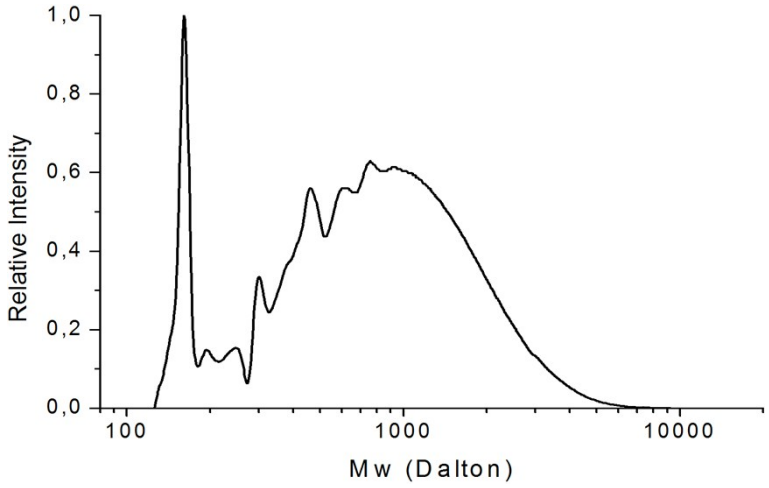

Figure S23. GPC (THF, against polystyrene standards) of kraft lignin (**L24**).

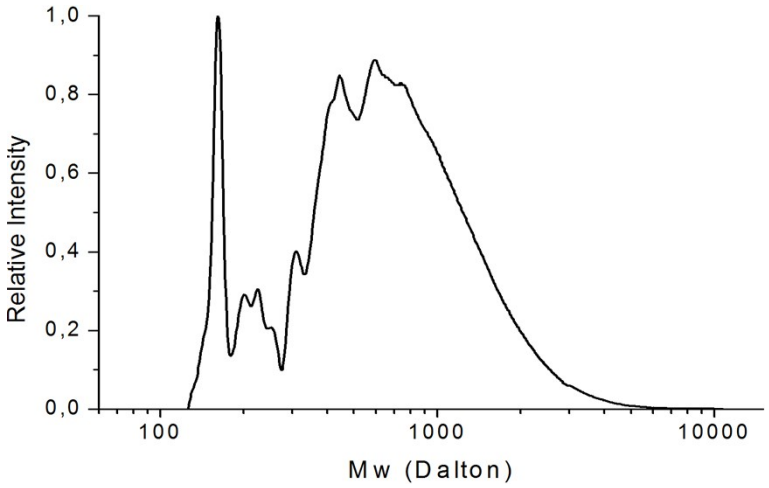

Figure S23. GPC (THF, against polystyrene standards) of soda protobind 1000 (**L26**).

Table S1. GPC data (THF, against polystyrene standards) of lignins **L1**-**L4**, **L6**-**L24** and **L26**.

Entry	Lignin #	Source and extraction method	GPC data		
			M_n (g/mol)	M_w (g/mol)	Đ
1	**L1**	Methansolv Walnut (Proc 1)	688	1518	2.2
2	**L2**	**L1** DCM soluble fraction	808	1510	1.9
3	**L3**	**L2** DCM insoluble fraction	1338	2734	2.0
4	**L4**	Methansolv Walnut (Proc 2)	1331	2333	1.8
5	**L6**	Methanosolv Pine (Proc 1)	1075	2088	1.9
6	**L7**	Ethanosolv Walnut	1351	3146	2.3
7	**L8**	Ethanosolv Douglas Fir	1503	3146	2.1
8	**L9**	Butanosolv Walnut	1055	3279	3.1
9	**L10**	Butanosolv Beech	1053	3048	2.9
10	**L11**	Butanosolv Douglas Fir	977	2763	2.8
11	**L12**	Dioxosolv Walnut	951	2005	2.1
12	**L13**	Dioxosolv Pine Batch 1	1498	2600	1.7
13	**L14**	Dioxosolv Pine Batch 2	1488	3089	2.1
14	**L15**	Dioxosolv Oak	1031	2420	2.3
15	**L16**	Dioxosolv Barley Straw	896	1794	2.0
16	**L17**	Dioxosolv Birch	1172	2756	2.4
17	**L18**	Fomic/acetic acid Oak	1574	2709	1.7
18	**L19**	Techn. Ethanosolv Beech	928	2016	2.2
19	**L20**	Techn. Ethanosolv Poplar	879	1681	1.9
20	**L21**	Techn. Ethanosolv Spruce	895	1847	2.1
21	**L22**	Techn. Alcell	631	1400	2.2
22	**L23**	Indulin-AT	527	985	1.9
23	**L24**	Kraft lignin	516	986	1.9
24	**L26**	Soda protobind 1000	467	777	1.7

2.1 2D-HSQC of lignins

2D-HSQC NMR spectra were recorded of **L1**-**L24** and **L26**. **L25** and **L27** were excluded from NMR analysis due to insolubility. According to common practice semi-quantitative analysis of the HSQC NMR spectra was performed by volume integration of the benzylic signals for the lignin linkages relative to the $S_{2,6}$, G_2 and $H_{2,6}$ aromatic resonances (logically adjusted for the number of protons). Several of these spectra have already been provided in earlier manuscript (see experimental section of the manuscript for references). For new lignin materials or for those for which no literature data was available, the spectra are shown below.

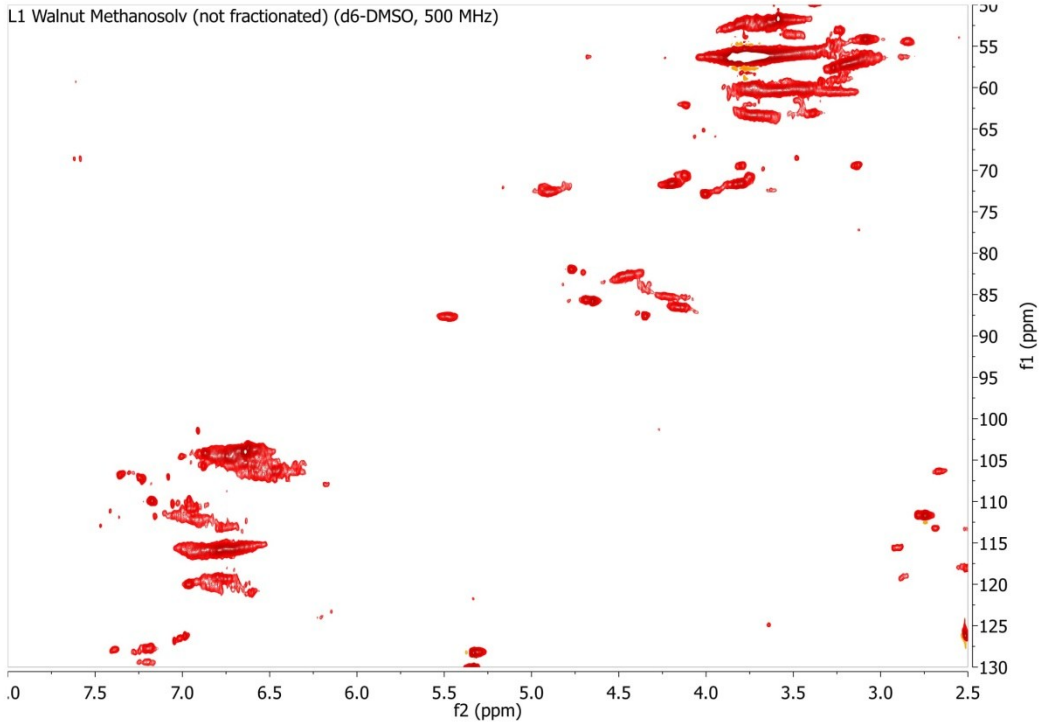

Figure S24 2D HSQC NMR spectrum (d_6-DMSO, 500 MHz, ^{13}C dimension SW 47-133 ppm, displayed 50-130 ppm) of walnut shell methanosolv lignin **L1** (procedure 1).

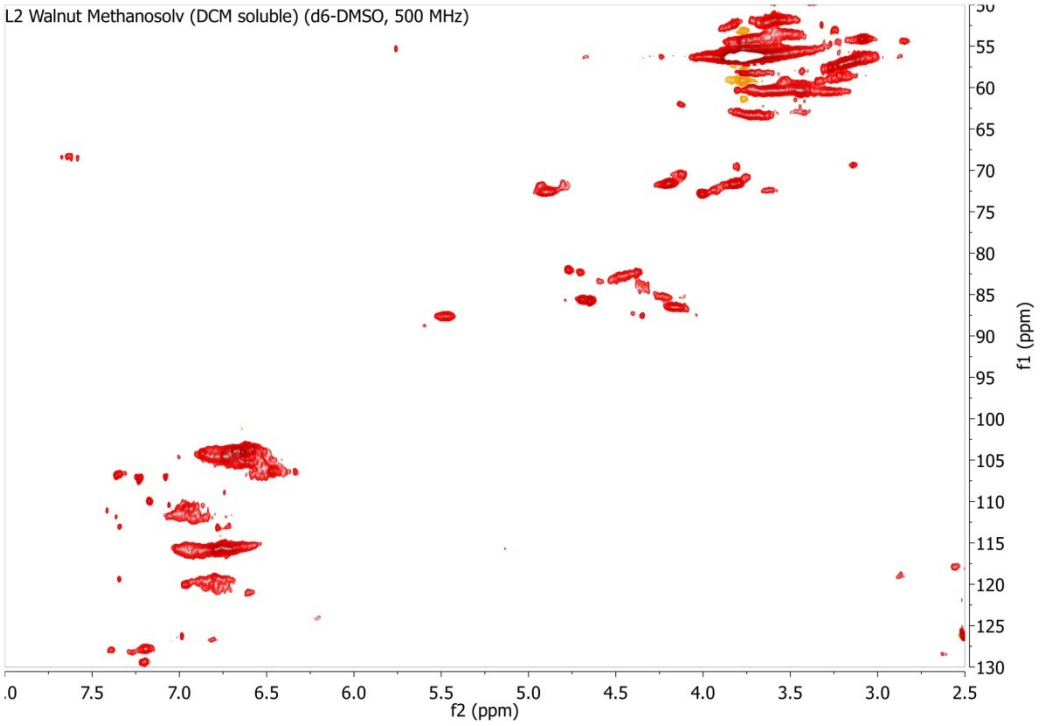

Figure S25 2D HSQC NMR spectrum (d_6-DMSO, 500 MHz, ^{13}C dimension SW 47-133 ppm, displayed 50-130 ppm) of the DCM soluble lignin fraction **L2** obtained of from walnut shell methanosolv lignin **L1**.

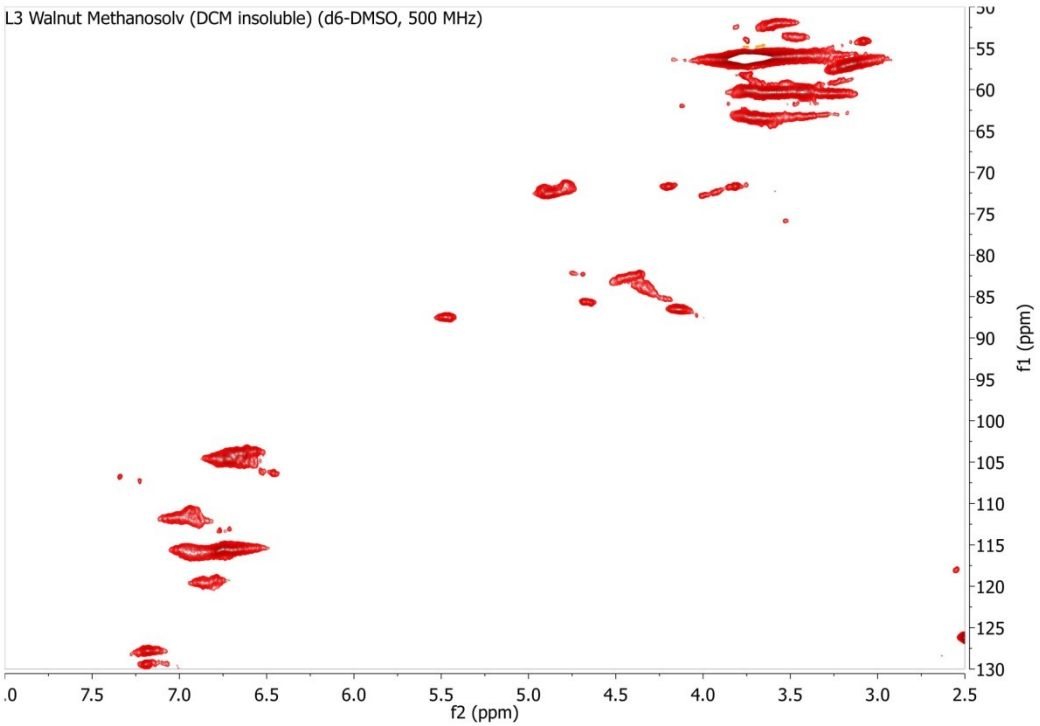

Figure S26 2D HSQC NMR spectrum (d_6-DMSO, 500 MHz, ^{13}C dimension SW 47-133 ppm, displayed 50-130 ppm) of the DCM insoluble lignin fraction **L3** obtained of from walnut shell methanosolv lignin **L1**.

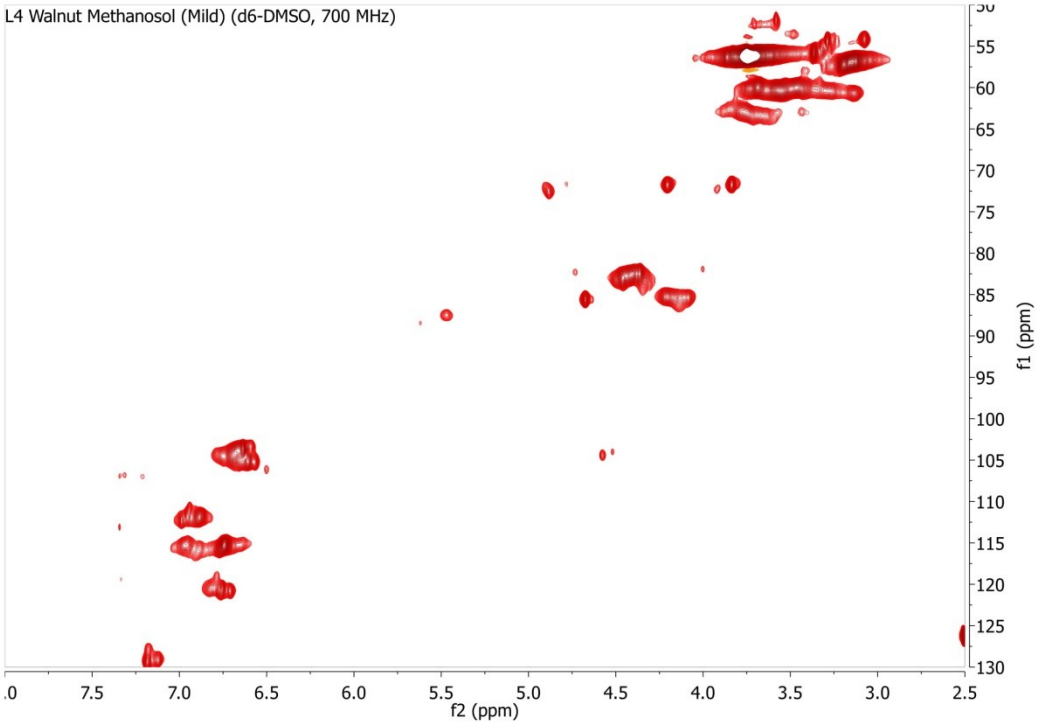

Figure S27 2D HSQC NMR spectrum (d_6-DMSO, 700 MHz, ^{13}C dimension SW 47-133 ppm, displayed 50-130 ppm) of walnut shell methanosolv lignin **L4** (procedure 2).

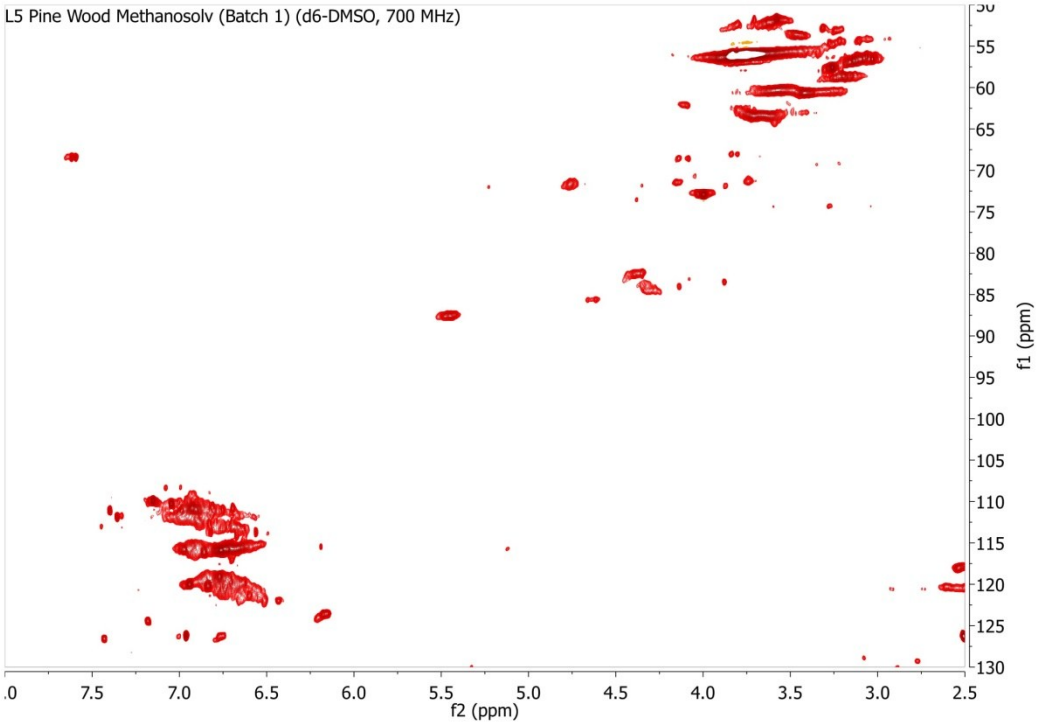

Figure S28 2D HSQC NMR spectrum (d_6-DMSO, 700 MHz, ^{13}C dimension SW 47-133 ppm, displayed 50-130 ppm) of pine wood methanosolv lignin **L5** (procedure 1).

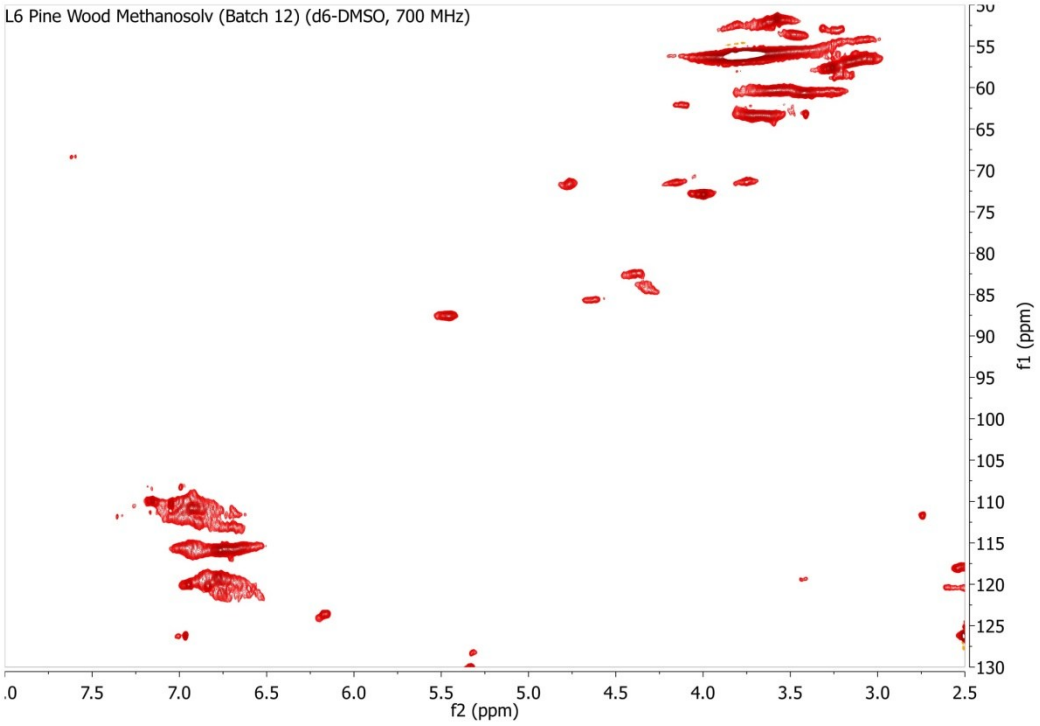

Figure S29 2D HSQC NMR spectrum (d_6-DMSO, 700 MHz, ^{13}C dimension SW 47-133 ppm, displayed 50-130 ppm) of pine wood methanosolv lignin **L6** (procedure 1).

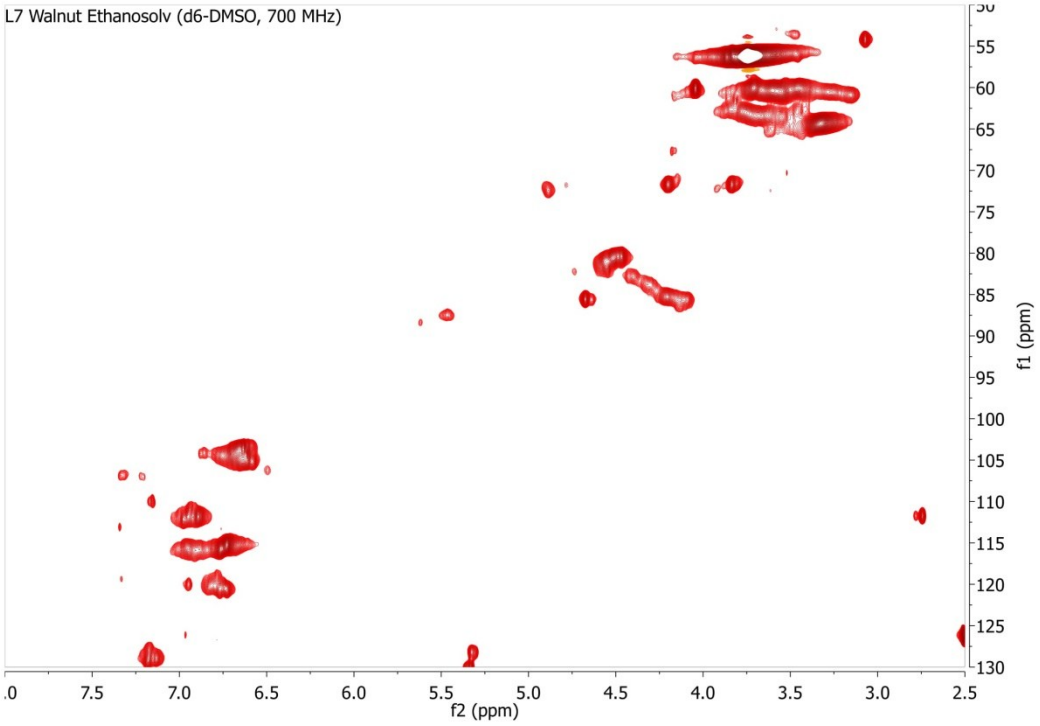

Figure S30 2D HSQC NMR spectrum (d_6-DMSO, 700 MHz, ^{13}C dimension SW 47-133 ppm, displayed 50-130 ppm) of walnut shell ethanosolv lignin **L7**.

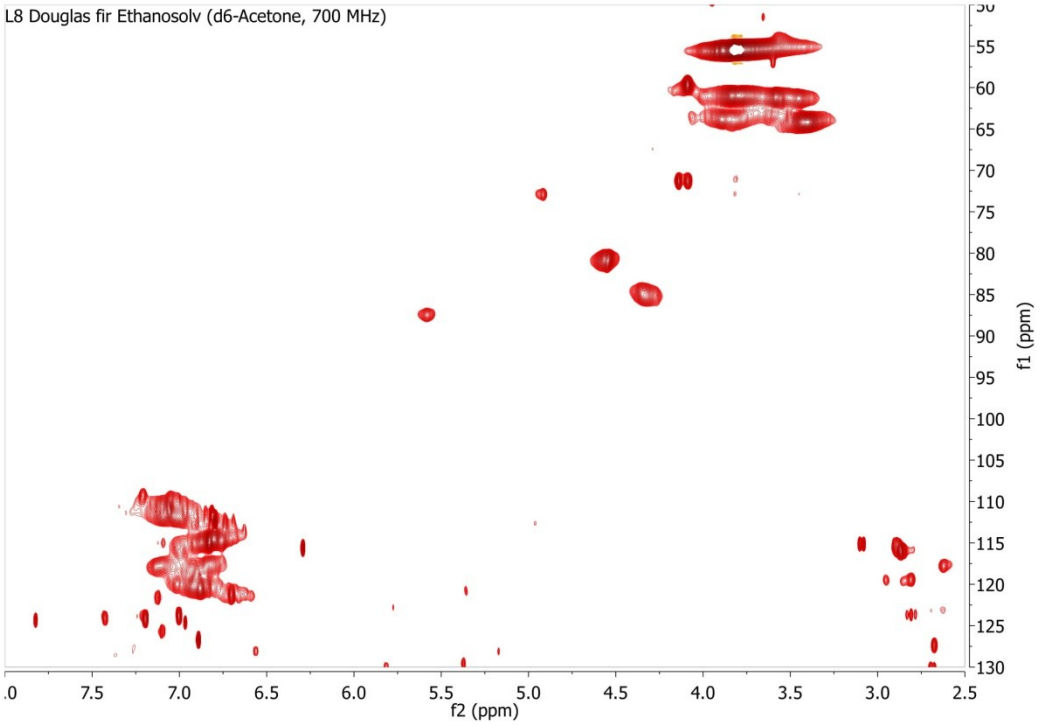

Figure S31 2D HSQC NMR spectrum (d_6-Acetone, 700 MHz, ^{13}C dimension SW 47-133 ppm, displayed 50-130 ppm) of Douglas fir ethanosolv lignin **L8**.

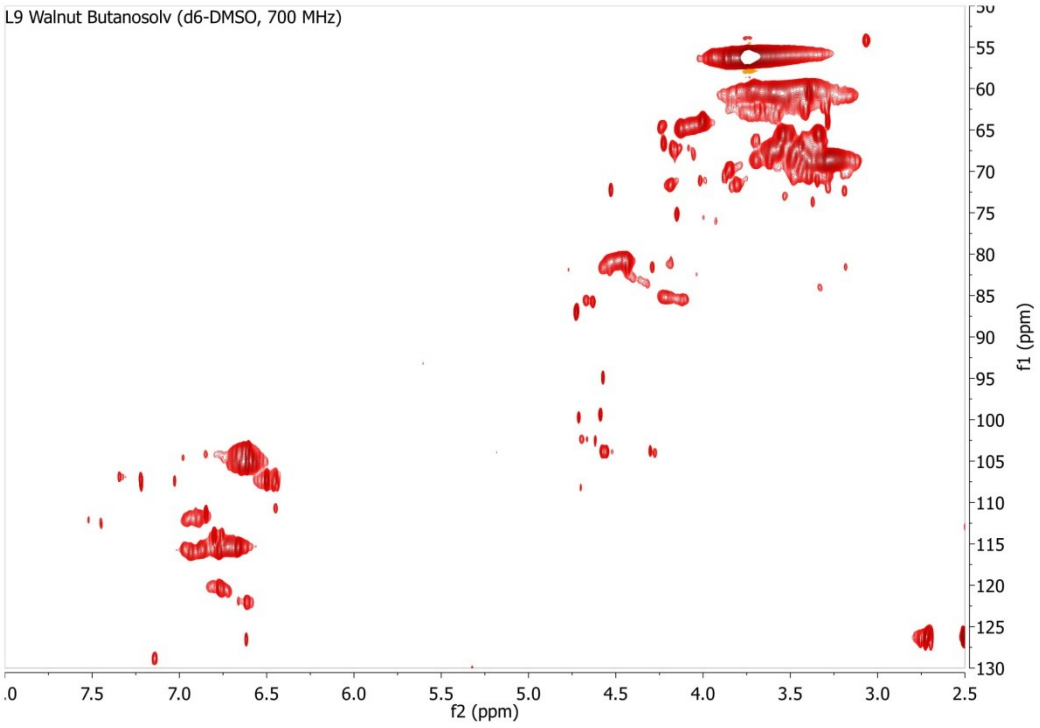

Figure S32 2D HSQC NMR spectrum (d_6-DMSO, 700 MHz, ^{13}C dimension SW 47-133 ppm, displayed 50-130 ppm) of walnut shell butanosolv lignin **L9**.

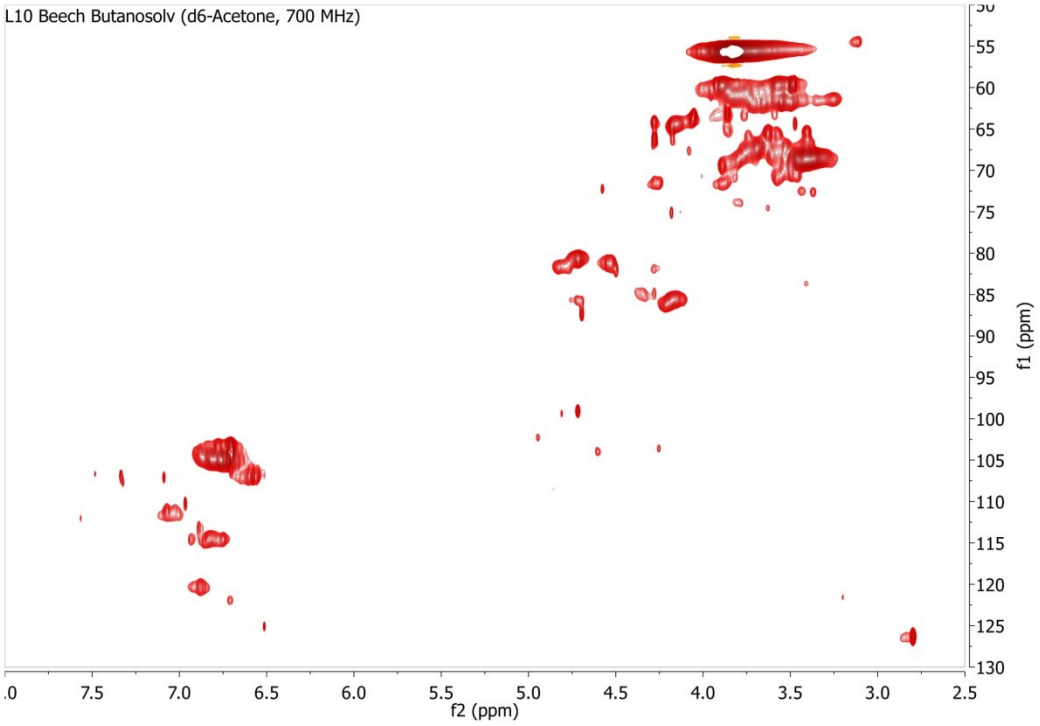

Figure S33 2D HSQC NMR spectrum (d_6-Acetone, 700 MHz, ^{13}C dimension SW 47-133 ppm, displayed 50-130 ppm) of beech butanosolv lignin **L10**.

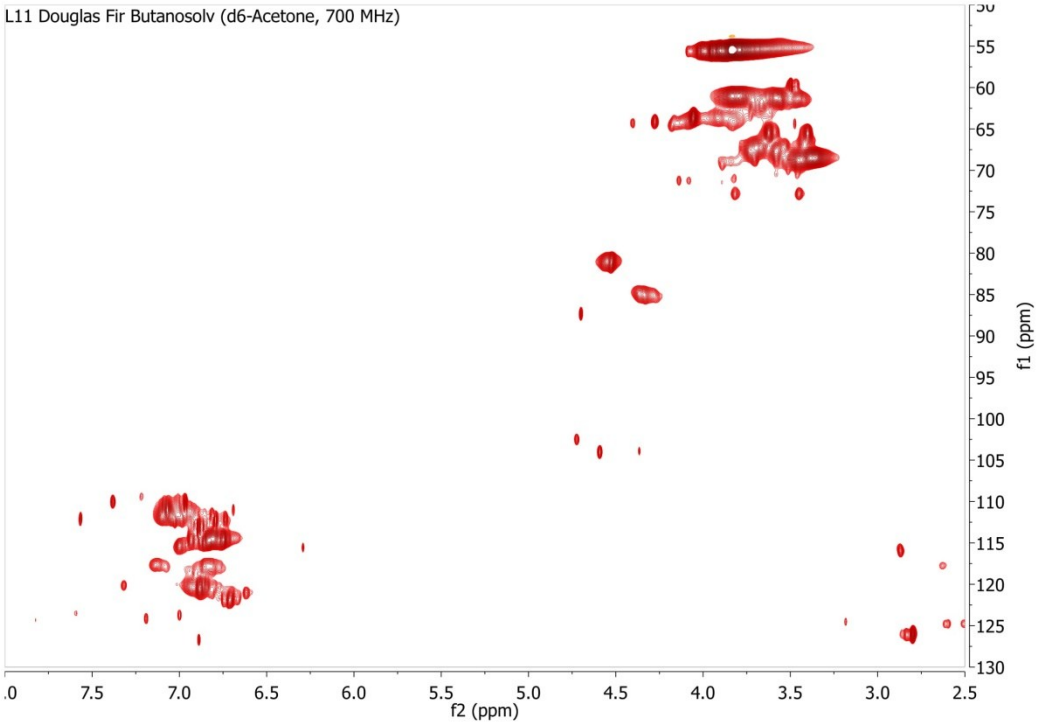

Figure S34 2D HSQC NMR spectrum (d_6-DMSO, 700 MHz, ^{13}C dimension SW 47-133 ppm, displayed 50-130 ppm) of Douglas fir butanosolv lignin **L11**.

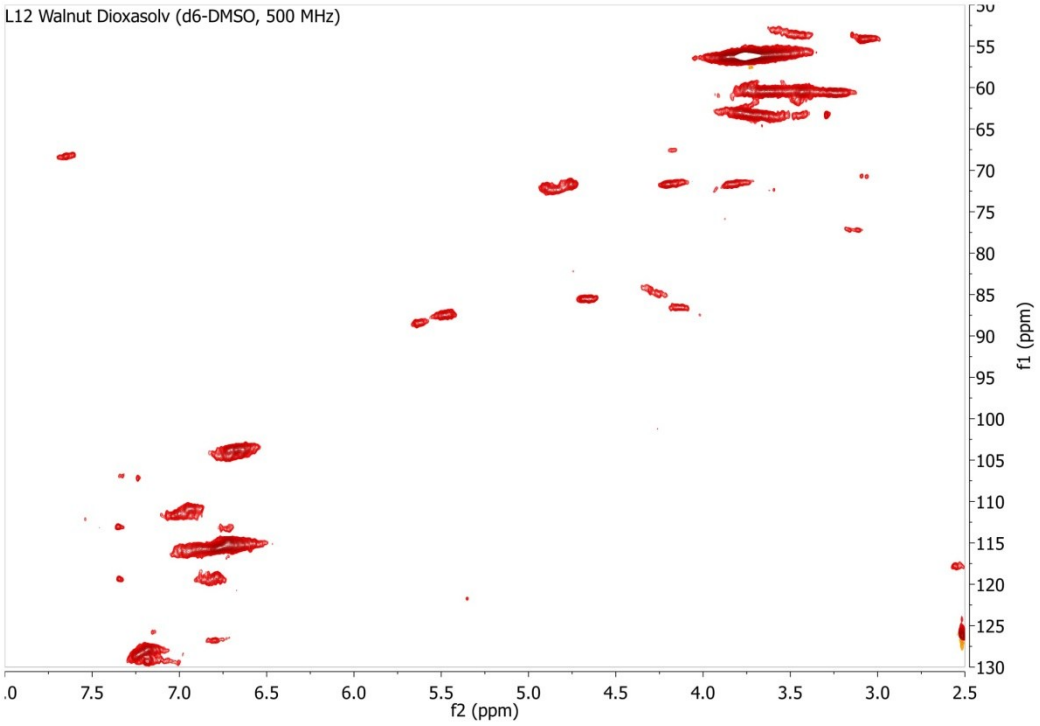

Figure S35 2D HSQC NMR spectrum (d_6-DMSO, 500 MHz, ^{13}C dimension SW 47-133 ppm, displayed 50-130 ppm) of walnut dioxosolv lignin **L12**.

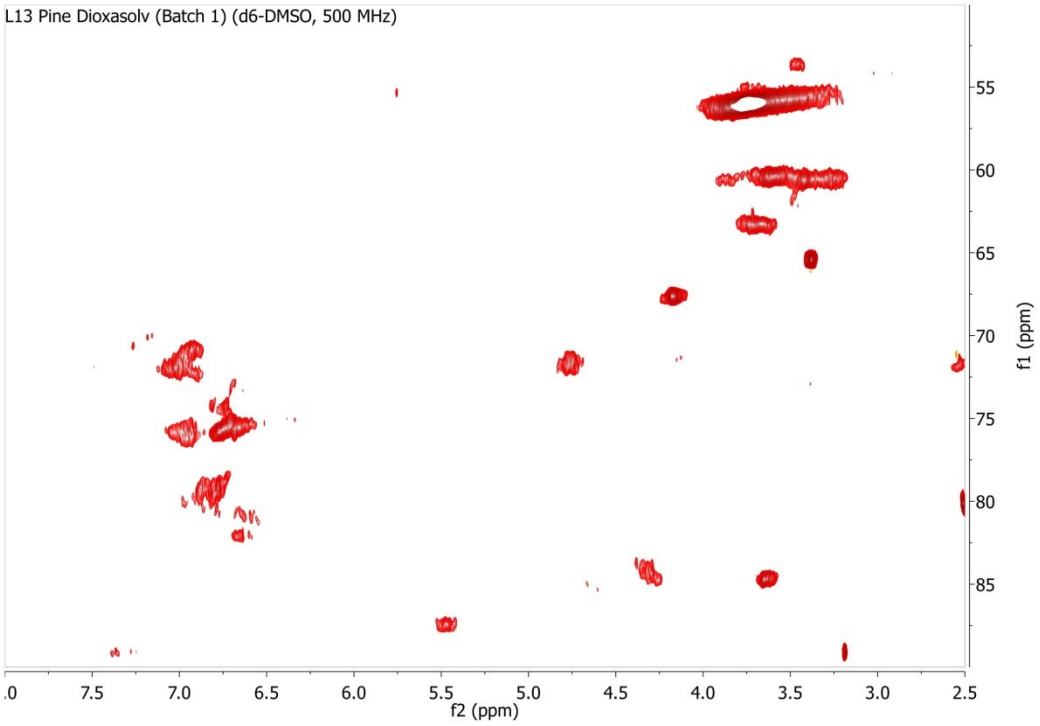

Figure S36 2D HSQC NMR spectrum (d_6-DMSO, 500 MHz, ^{13}C dimension SW 50-90 ppm, displayed 50-90 ppm) of pine dioxosolv lignin **L13**.

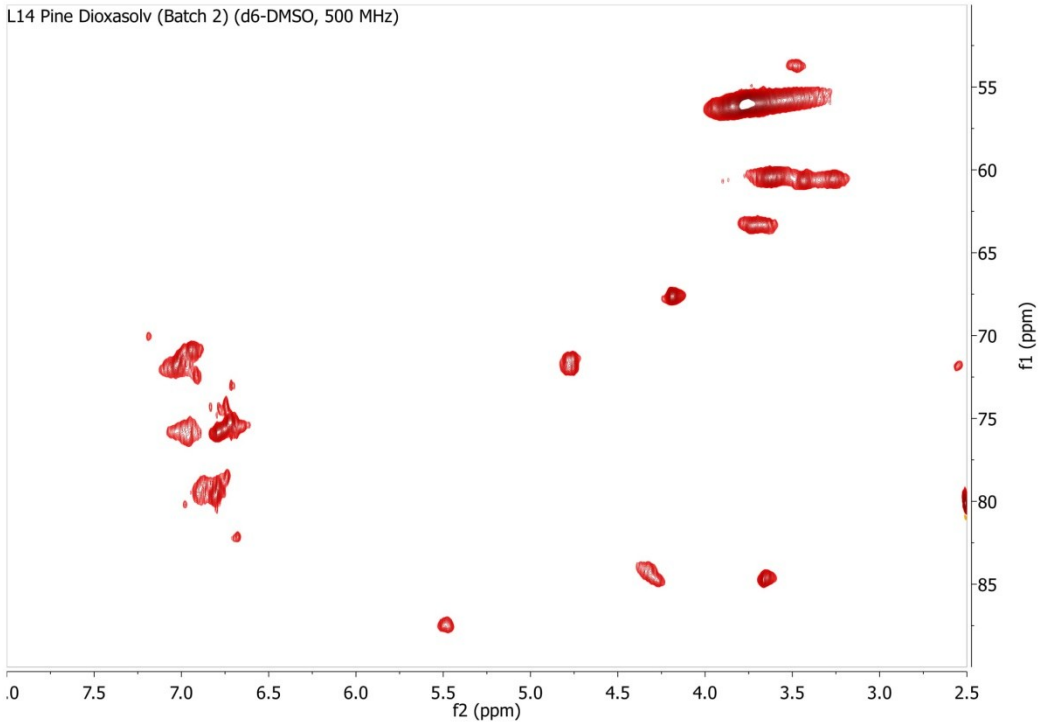

Figure S37 2D HSQC NMR spectrum (d_6-DMSO, 500 MHz, ^{13}C dimension SW 50-90 ppm, displayed 50-90 ppm) of pine dioxosolv lignin **L14**.

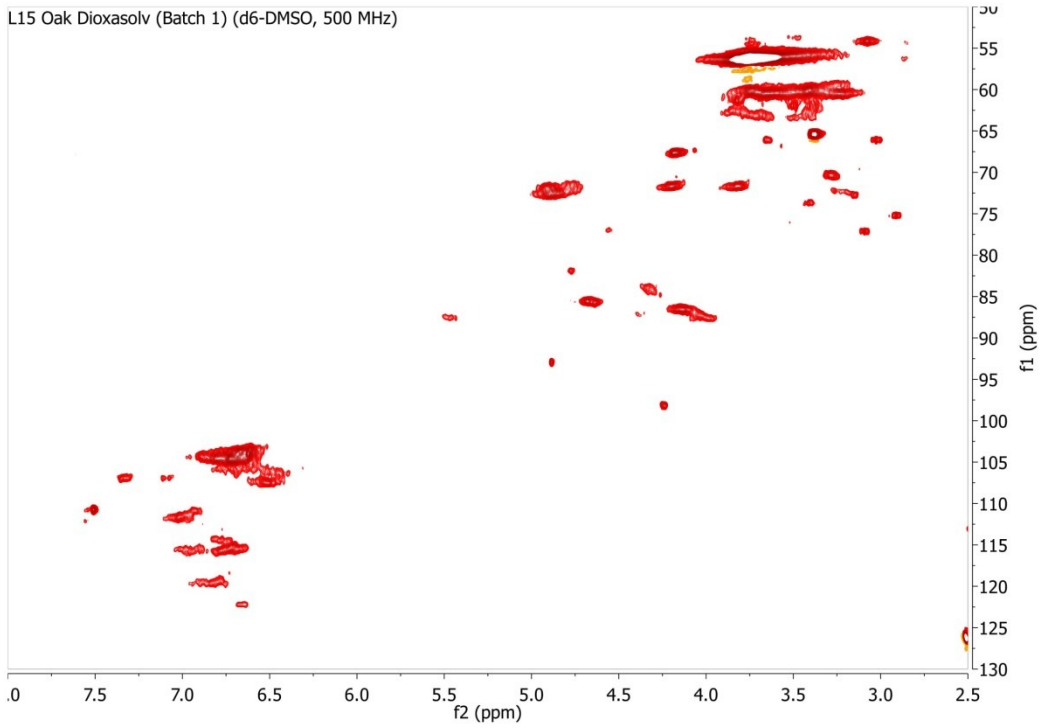

Figure S38 2D HSQC NMR spectrum (d_6-DMSO, 500 MHz, ^{13}C dimension SW 47-133 ppm, displayed 50-130 ppm) of oak dioxosolv lignin **L15**.

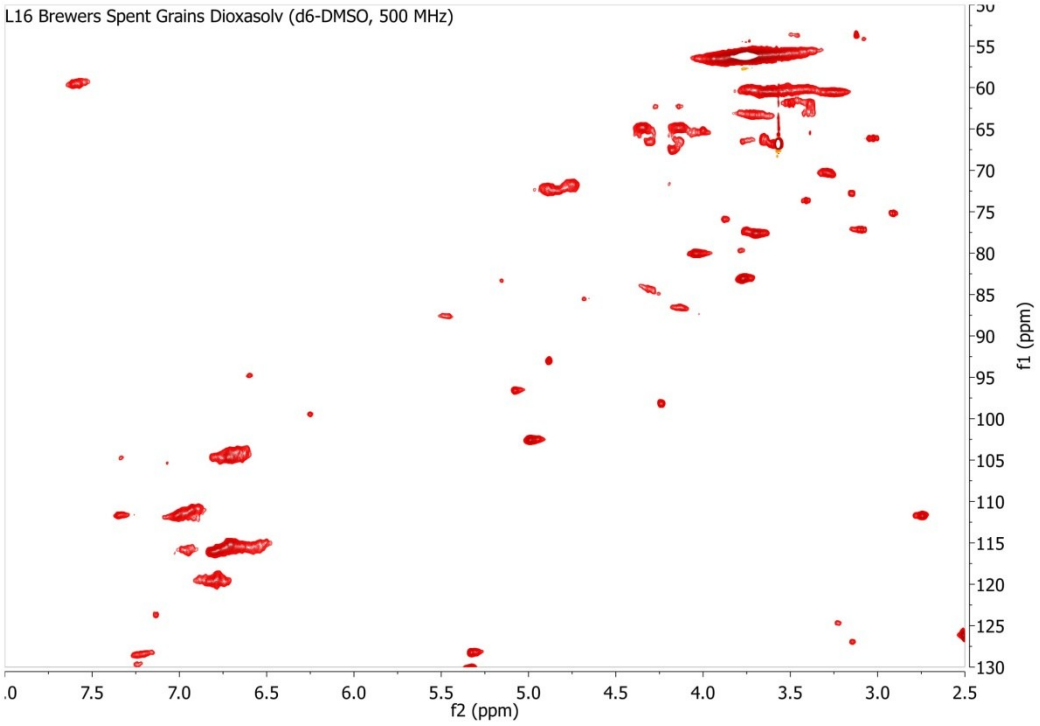

Figure S39 2D HSQC NMR spectrum (d_6-DMSO, 500 MHz, ^{13}C dimension SW 47-133 ppm, displayed 50-130 ppm) of Brewers Spent Grain (Barley) dioxosolv lignin **L16**.

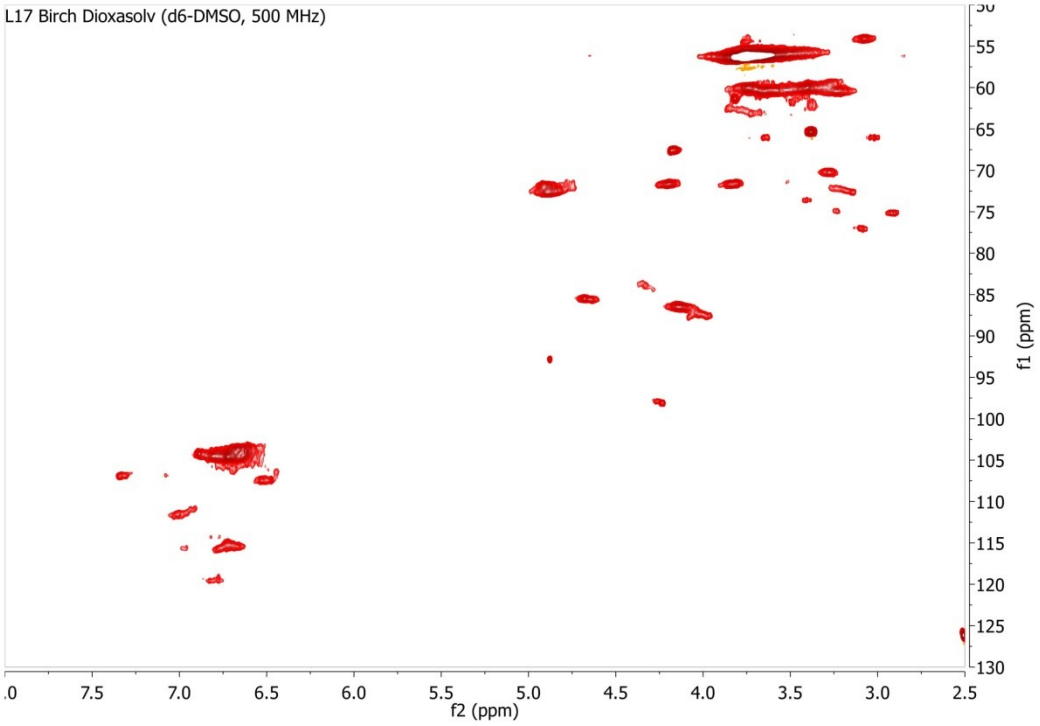

Figure S40 2D HSQC NMR spectrum (d_6-DMSO, 500 MHz, ^{13}C dimension SW 47-133 ppm, displayed 50-130 ppm) of Birch dioxosolv lignin **L17**.

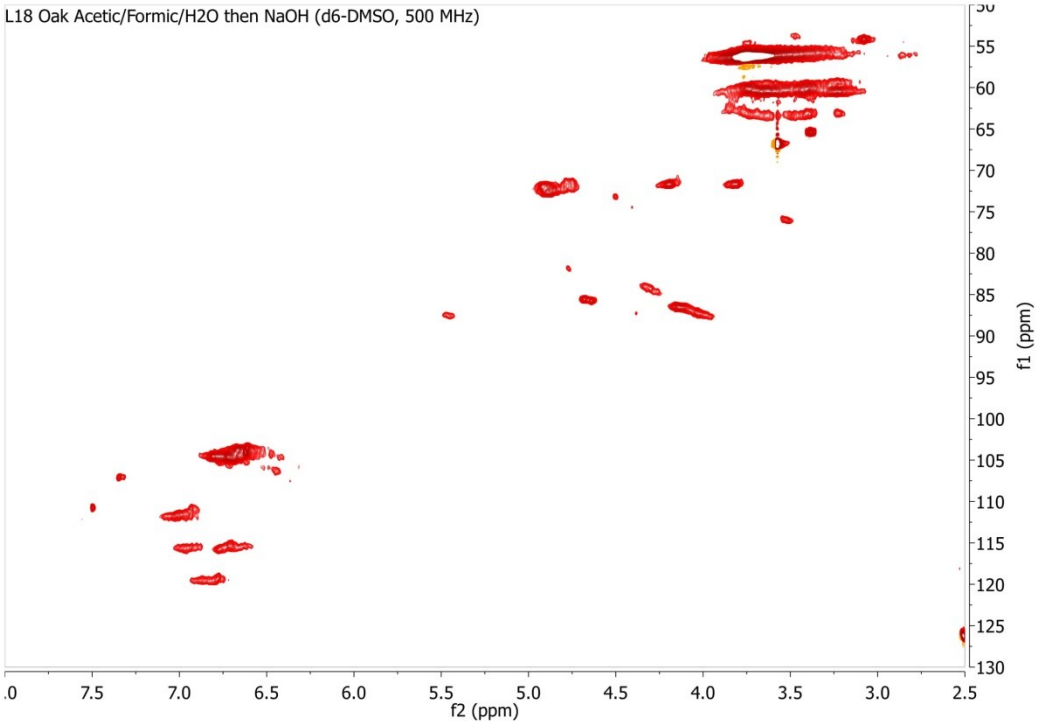

Figure S41 2D HSQC NMR spectrum (d_6-DMSO, 500 MHz, ^{13}C dimension SW 47-133 ppm, displayed 50-130 ppm) of oak acetic/formic acid/water then NaOH lignin **L18**.

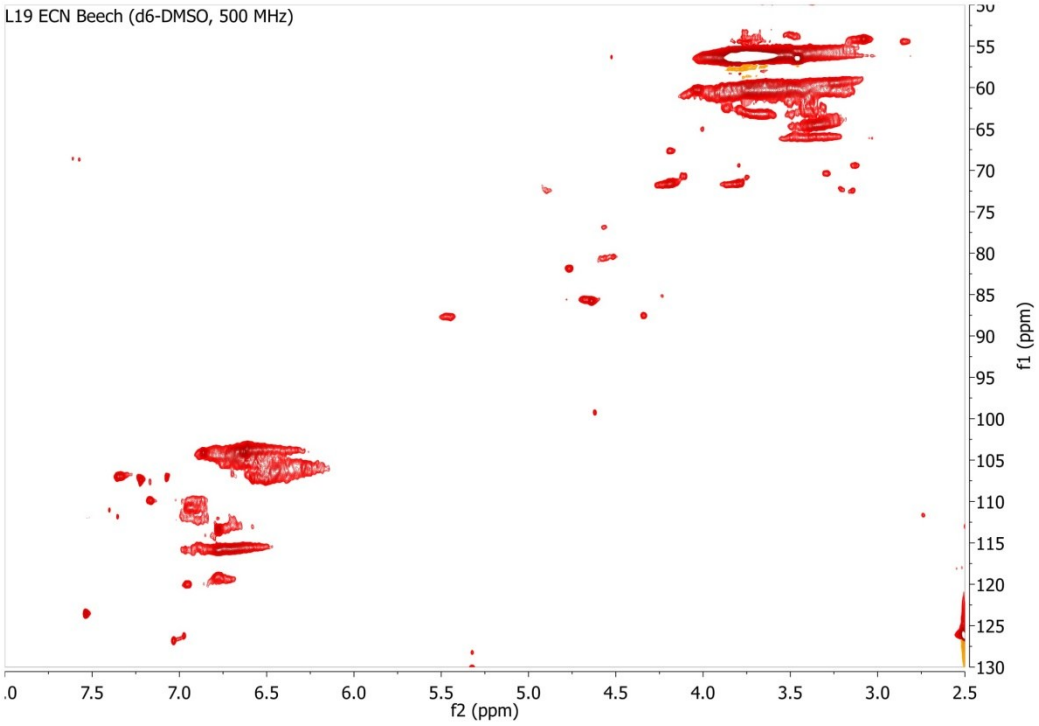

Figure S42 2D HSQC NMR spectrum (d_6-DMSO, 500 MHz, ^{13}C dimension SW 47-133 ppm, displayed 50-130 ppm) of technical ethanosolv beech lignin **L19**.

Table S2. Overview of lignin characteristics determined by 2D-HSQC NMR analysis (values rounded to nearest whole number)

Entry	Lignin	Description	relative %			per 100 C9 units						
			S	G	H	β-O-4-αOH	β-O-4-αOR	Total β-O-4	β-β	β-β'	β-5	HK
1	**L1**	Methansolv Walnut (Proc 1)	63	32	4	8	5	**13**	4	0	5	0
2	**L2**	**L1** DCM soluble fraction	65	29	6	14	12	**25**	6	5	8	0
3	**L3**	**L2** DCM insoluble fraction	45	38	17	32	16	**48**	3	0	11	0
4	**L4**	Methansolv Walnut (Proc 2)	47	42	11	8	54	**62**	5	0	9	1
5	**L5**	Methanosolv Pine (Proc 1)	0	100	0	6	5	**11**	1	0	10	0
6	**L6**	Methanosolv Pine (Proc 1)	0	100	0	7	5	**12**	4	0	10	0
7	**L7**	Ethanosolv Walnut	47	41	12	8	50	**58**	5	0	10	2
8*	**L8**	Ethanosolv Douglas Fir	0	100	0	9	43	**52**	2	0	13	1
9	**L9**	Butanosolv Walnut	73	25	2	1	40	**41**	3	0	3	3
10*	**L10**	Butanosolv Beech	82	18	0	3	47	**50**	4	0	1	2
11*	**L11**	Butanosolv Douglas Fir	0	100	0	0	52	**52**	0	0	6	3
12	**L12**	Dioxosolv Walnut	31	38	31	23	0	**23**	6	0	22	2
13	**L13**	Dioxosolv Pine Batch 1	0	100	0	43	0	**43**	3	0	20	34
14	**L14**	Dioxosolv Pine Batch 2	0	100	0	33	0	**33**	3	0	18	17
15	**L15**	Dioxosolv Oak	84	16	0	41	0	**41**	6	2	3	9
16	**L16**	Dioxosolv Barley Straw	33	57	9	45	0	**45**	2	0	9	1
17	**L17**	Dioxosolv Birch	88	12	0	45	0	**45**	6	0	2	5
18	**L18**	Fomic/acetic acid Oak	74	26	0	43	0	**43**	5	2	4	0
19	**L19**	Techn. Ethanosolv Beech	68	32	0	5	6	**11**	3	3	3	0.5
20	**L20**	Techn. Ethanosolv Poplar	59	41	0	0	4	**4**	2	3	3	-
21	**L21**	Techn. Ethanosolv Spruce	0	100	0	0	2	**2**	1	0	5	-
22	**L22**	Techn. Alcell	66	34	0	8	5	**13**	3	2	2	-
23	**L23**	Indulin-AT	0	100	0	6	0	**6**	1	0	2	0
24	**L24**	Kraft	0	100	0	4	0	**4**	3	0	1	0
25	**L26**	Soda protobind 1000	48	40	12	3	0	**3**	1	0	1	0

* NMR analysis conducted using d_6-acetone

3. Lignin depolymerisation

3.1 GPC analysis of depolymerisation reactions at varying temperature and time

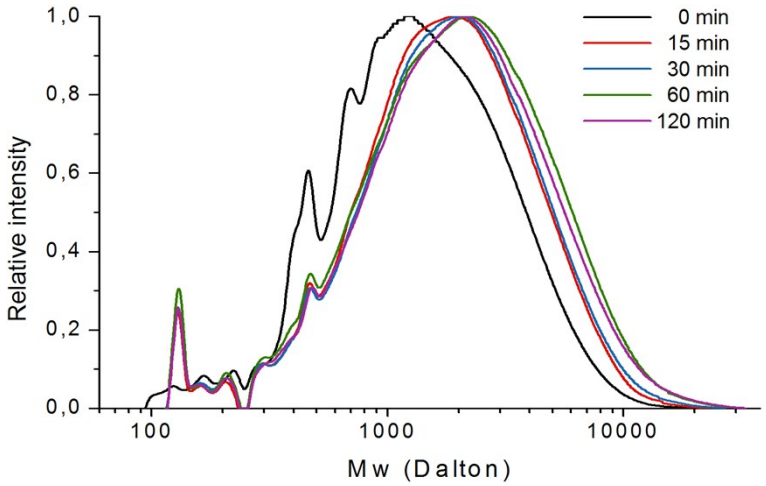

Figure S43. GPC (THF, against polystyrene standards) of residual fraction of the depolymerisation of **L19** at varying reaction times (140 °C, 10 wt% $Fe(OTf)_3$, 33 wt% ethylene glycol, 1,4-dioxane).

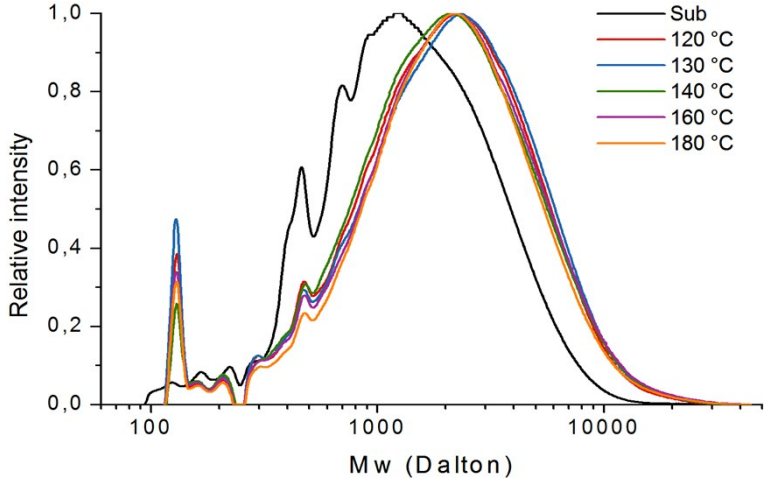

Figure S44. GPC (THF, against polystyrene standards) of residual fraction of the depolymerisation of **L19** at varying reaction temperatures (30 min, 10 wt% $Fe(OTf)_3$, 33 wt% ethylene glycol, 1,4-dioxane).

*3.2 GPC analysis of depolymerisation reactions of **L1**-**L27***

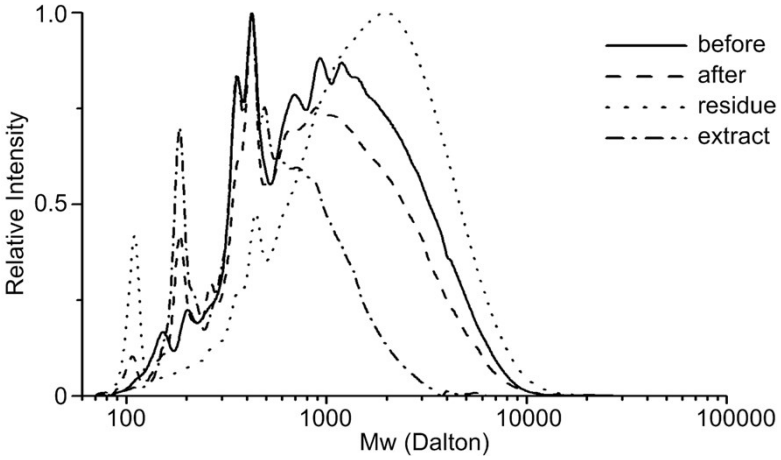

Figure S45. GPC (THF, against polystyrene standards) of different fraction obtained from the depolymerisation of **L1** (15 min, 10 wt% $Fe(OTf)_3$, 30 wt% ethylene glycol, 1,4-dioxane).

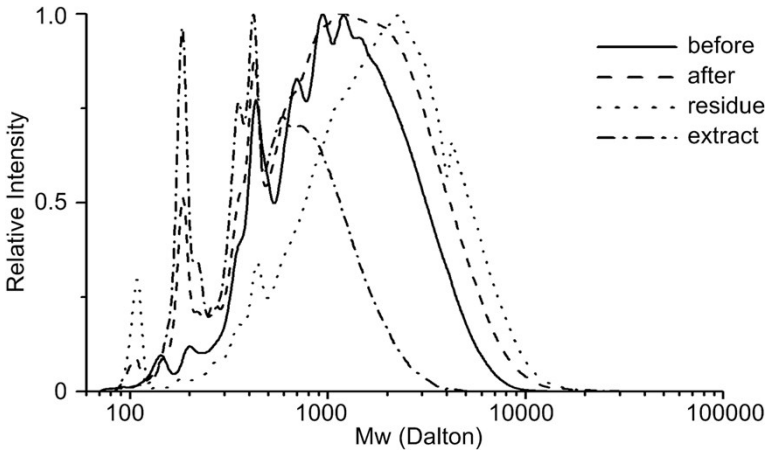

Figure S46. GPC (THF, against polystyrene standards) of different fraction obtained from the depolymerisation of **L2** (15 min, 10 wt% $Fe(OTf)_3$, 30 wt% ethylene glycol, 1,4-dioxane).

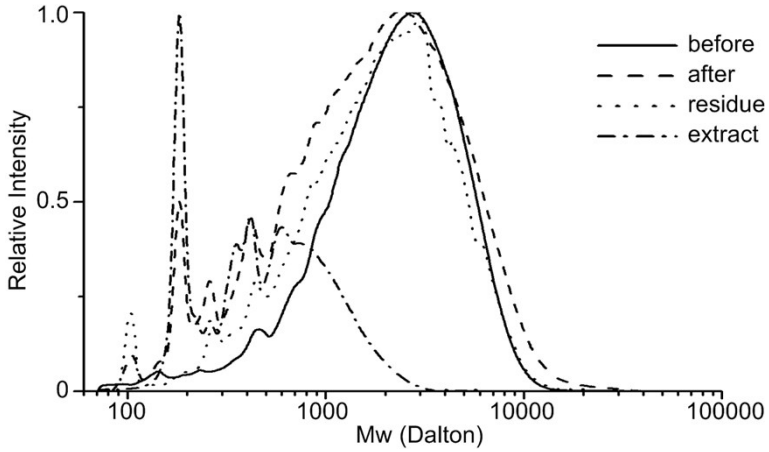

Figure S47. GPC (THF, against polystyrene standards) of different fraction obtained from the depolymerisation of **L3** (15 min, 10 wt% $Fe(OTf)_3$, 30 wt% ethylene glycol, 1,4-dioxane).

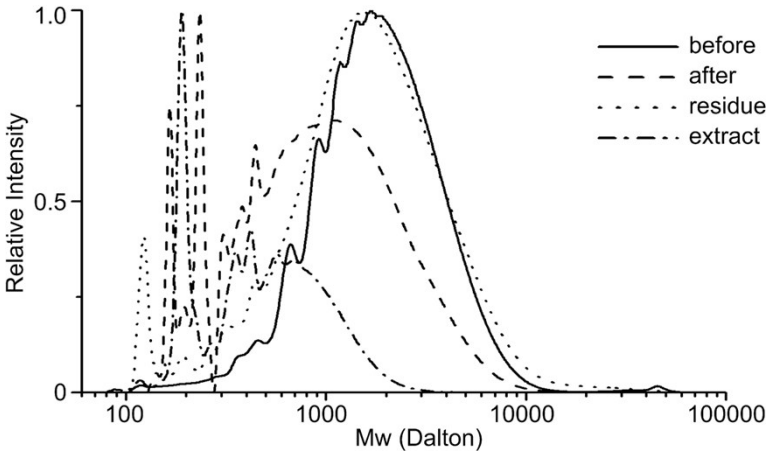

Figure S48. GPC (THF, against polystyrene standards) of different fraction obtained from the depolymerisation of **L4** (15 min, 10 wt% $Fe(OTf)_3$, 30 wt% ethylene glycol, 1,4-dioxane).

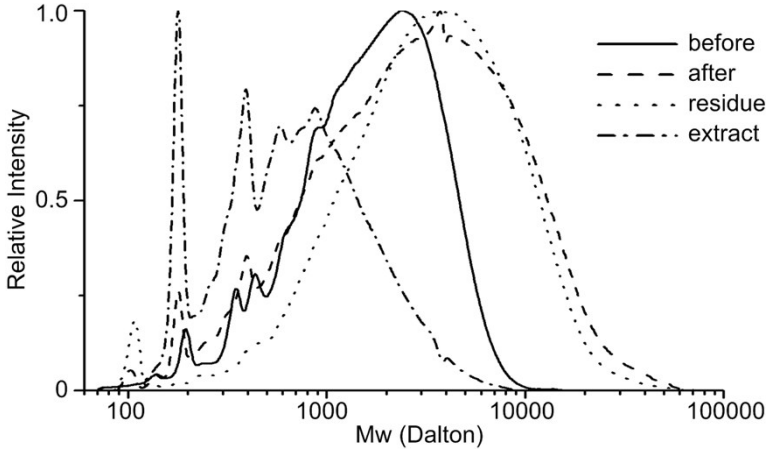

Figure S49. GPC (THF, against polystyrene standards) of different fraction obtained from the depolymerisation of **L5** (15 min, 10 wt% $Fe(OTf)_3$, 30 wt% ethylene glycol, 1,4-dioxane).

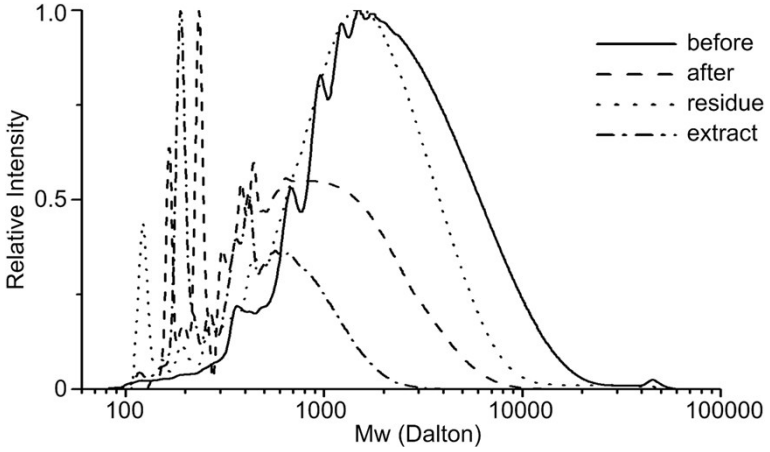

Figure S50. GPC (THF, against polystyrene standards) of different fraction obtained from the depolymerisation of **L7** (15 min, 10 wt% $Fe(OTf)_3$, 30 wt% ethylene glycol, 1,4-dioxane).

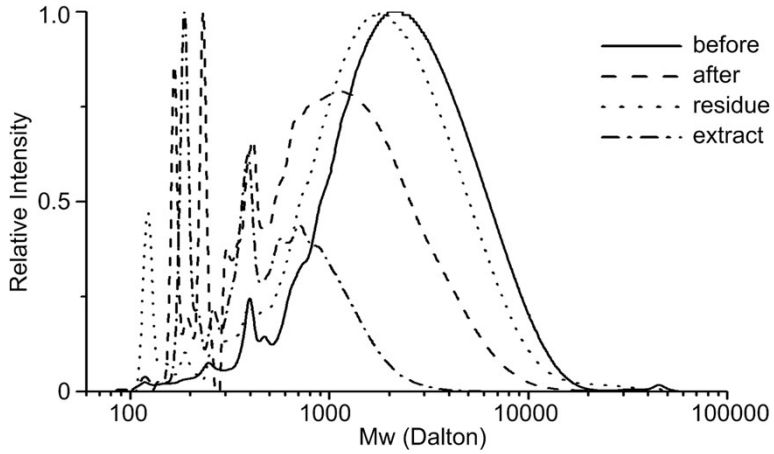

Figure S51. GPC (THF, against polystyrene standards) of different fraction obtained from the depolymerisation of **L8** (15 min, 10 wt% $Fe(OTf)_3$, 30 wt% ethylene glycol, 1,4-dioxane).

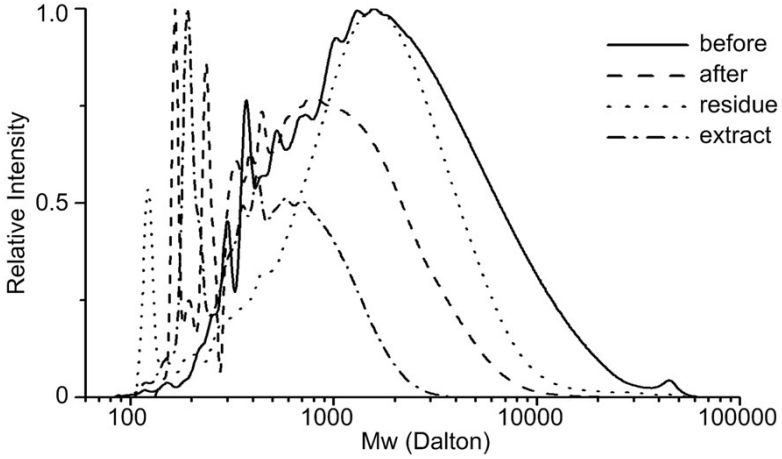

Figure S52. GPC (THF, against polystyrene standards) of different fraction obtained from the depolymerisation of **L9** (15 min, 10 wt% $Fe(OTf)_3$, 30 wt% ethylene glycol, 1,4-dioxane).

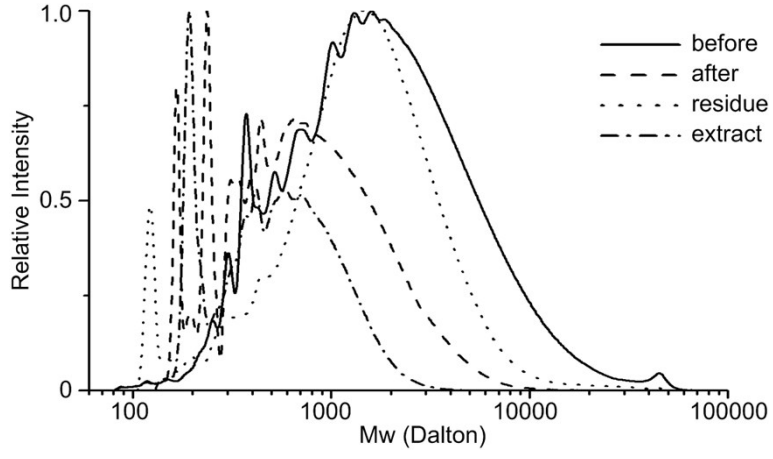

Figure S53. GPC (THF, against polystyrene standards) of different fraction obtained from the depolymerisation of **L10** (15 min, 10 wt% $Fe(OTf)_3$, 30 wt% ethylene glycol, 1,4-dioxane).

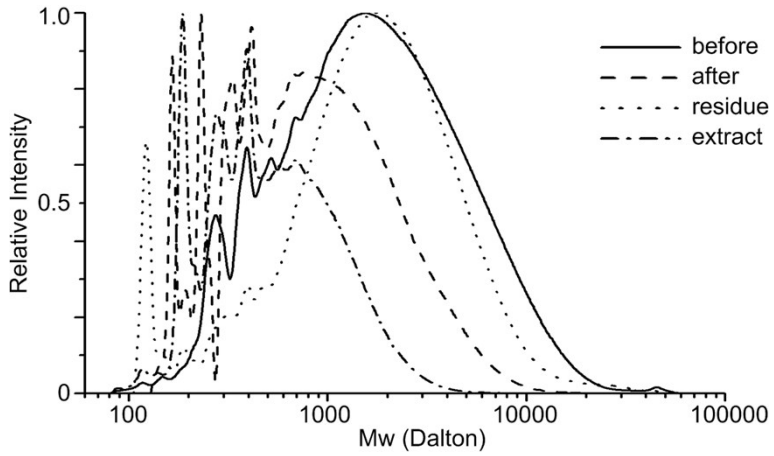

Figure S54. GPC (THF, against polystyrene standards) of different fraction obtained from the depolymerisation of **L11** (15 min, 10 wt% $Fe(OTf)_3$, 30 wt% ethylene glycol, 1,4-dioxane).

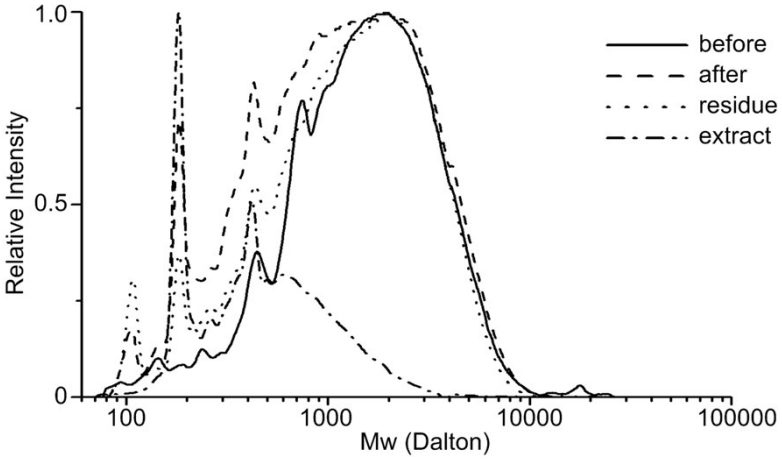

Figure S55. GPC (THF, against polystyrene standards) of different fraction obtained from the depolymerisation of **L12** (15 min, 10 wt% $Fe(OTf)_3$, 30 wt% ethylene glycol, 1,4-dioxane).

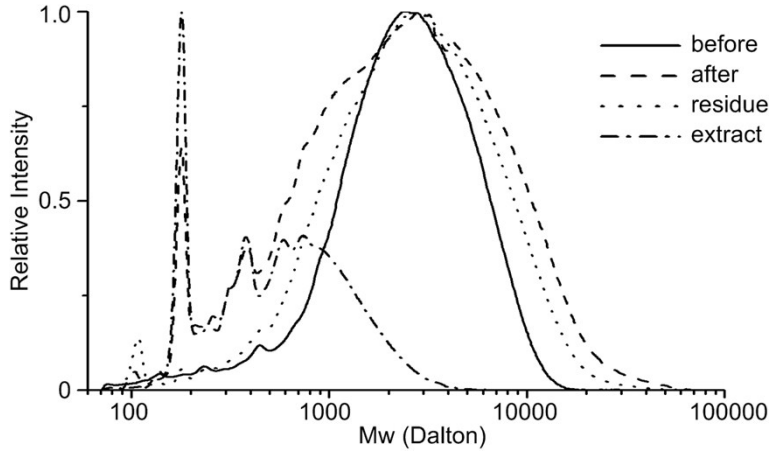

Figure S56. GPC (THF, against polystyrene standards) of different fraction obtained from the depolymerisation of **L13** (15 min, 10 wt% $Fe(OTf)_3$, 30 wt% ethylene glycol, 1,4-dioxane).

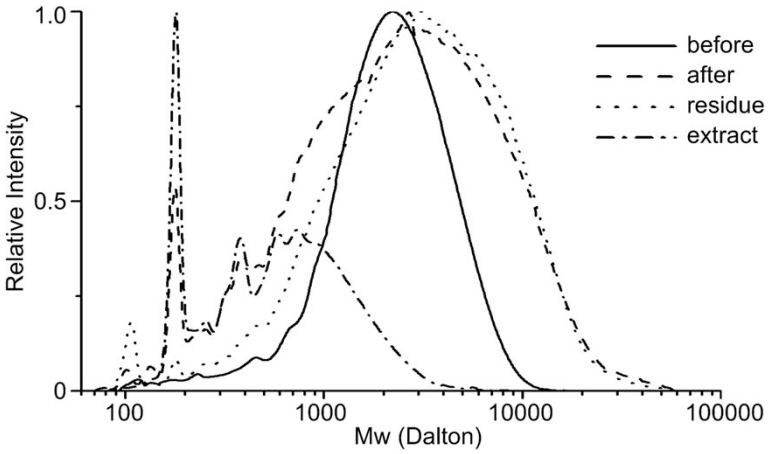

Figure S57. GPC (THF, against polystyrene standards) of different fraction obtained from the depolymerisation of **L14** (15 min, 10 wt% $Fe(OTf)_3$, 30 wt% ethylene glycol, 1,4-dioxane).

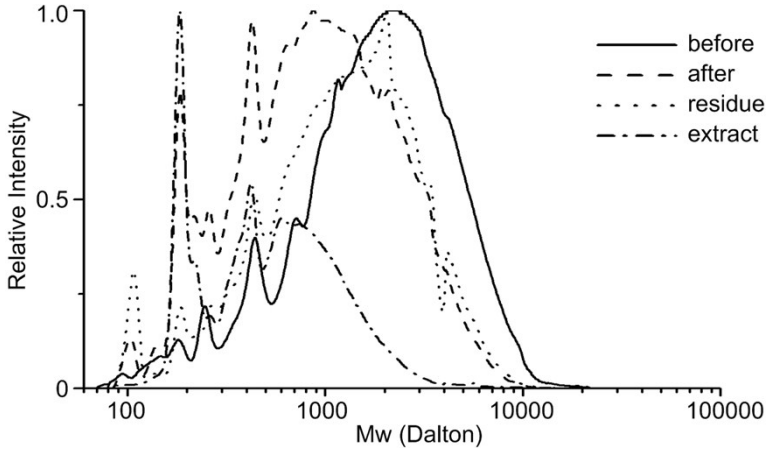

Figure S58. GPC (THF, against polystyrene standards) of different fraction obtained from the depolymerisation of **L15** (15 min, 10 wt% $Fe(OTf)_3$, 30 wt% ethylene glycol, 1,4-dioxane).

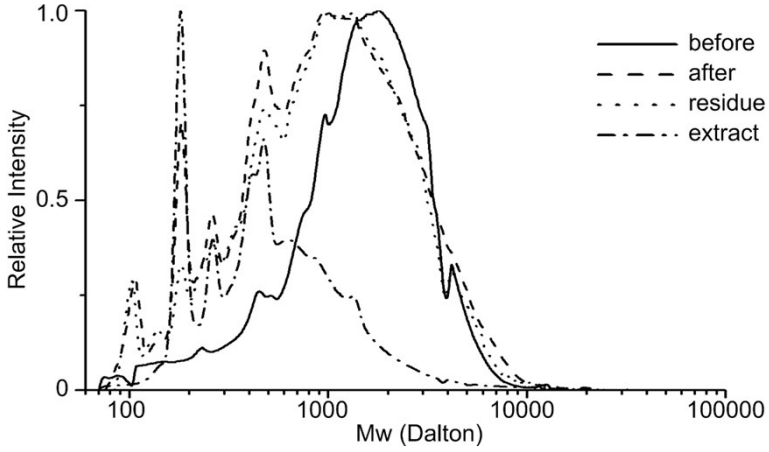

Figure S59. GPC (THF, against polystyrene standards) of different fraction obtained from the depolymerisation of **L16** (15 min, 10 wt% $Fe(OTf)_3$, 30 wt% ethylene glycol, 1,4-dioxane).

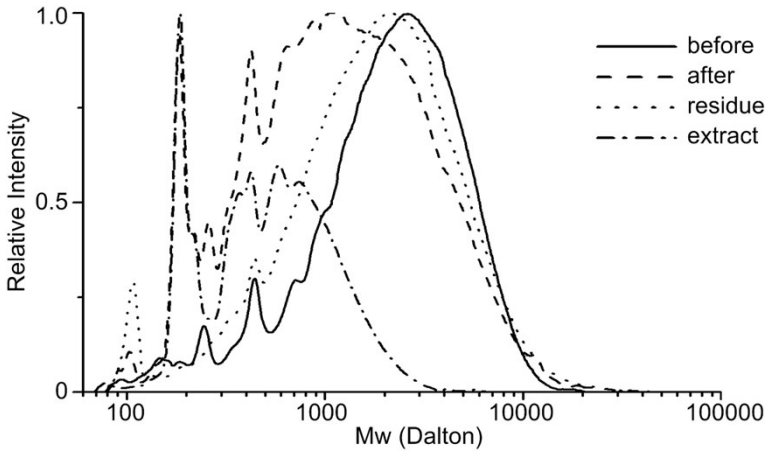

Figure S60. GPC (THF, against polystyrene standards) of different fraction obtained from the depolymerisation of **L17** (15 min, 10 wt% $Fe(OTf)_3$, 30 wt% ethylene glycol, 1,4-dioxane).

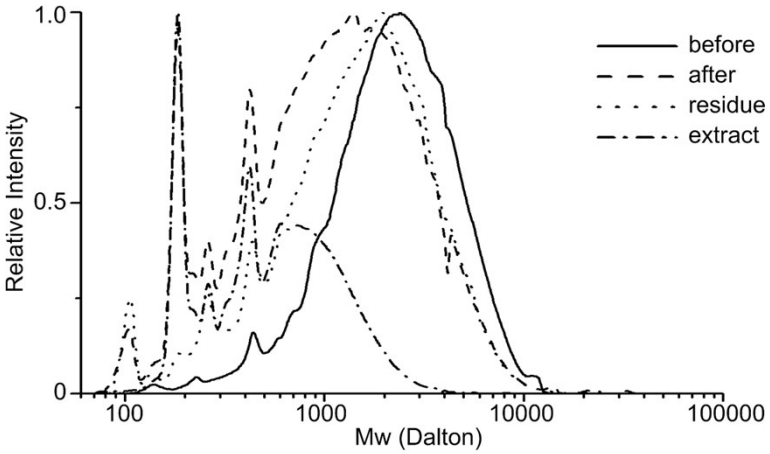

Figure S61. GPC (THF, against polystyrene standards) of different fraction obtained from the depolymerisation of **L18** (15 min, 10 wt% $Fe(OTf)_3$, 30 wt% ethylene glycol, 1,4-dioxane).

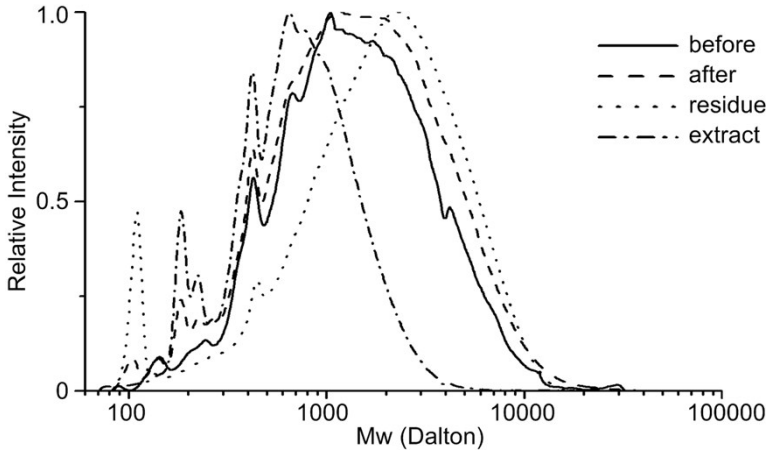

Figure S62. GPC (THF, against polystyrene standards) of different fraction obtained from the depolymerisation of **L19** (15 min, 10 wt% $Fe(OTf)_3$, 30 wt% ethylene glycol, 1,4-dioxane).

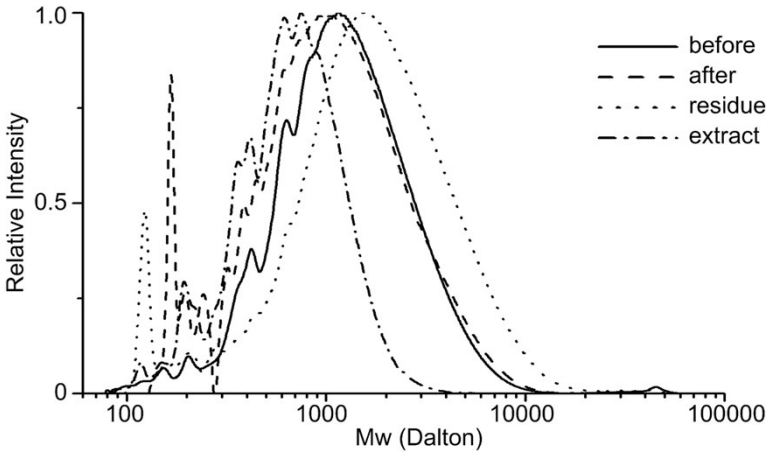

Figure S63. GPC (THF, against polystyrene standards) of different fraction obtained from the depolymerisation of **L20** (15 min, 10 wt% $Fe(OTf)_3$, 30 wt% ethylene glycol, 1,4-dioxane).

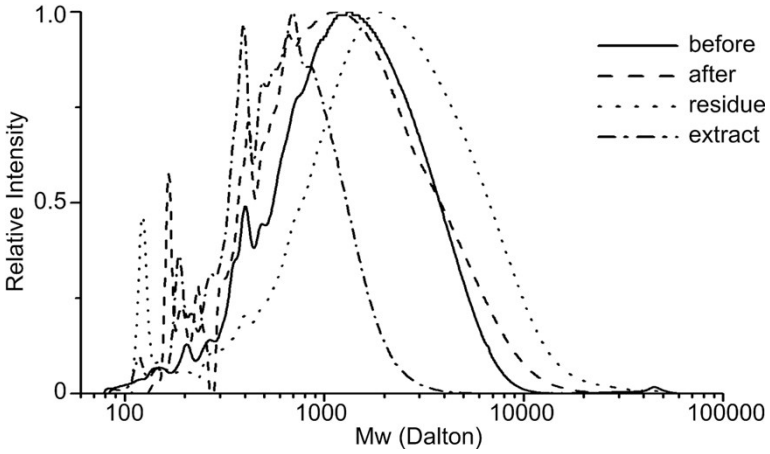

Figure S64. GPC (THF, against polystyrene standards) of different fraction obtained from the depolymerisation of **L21** (15 min, 10 wt% $Fe(OTf)_3$, 30 wt% ethylene glycol, 1,4-dioxane).

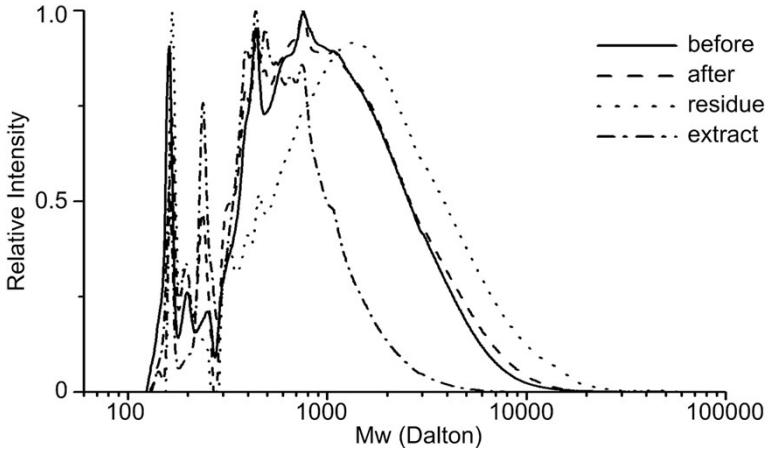

Figure S65. GPC (THF, against polystyrene standards) of different fraction obtained from the depolymerisation of **L22** (15 min, 10 wt% $Fe(OTf)_3$, 30 wt% ethylene glycol, 1,4-dioxane).

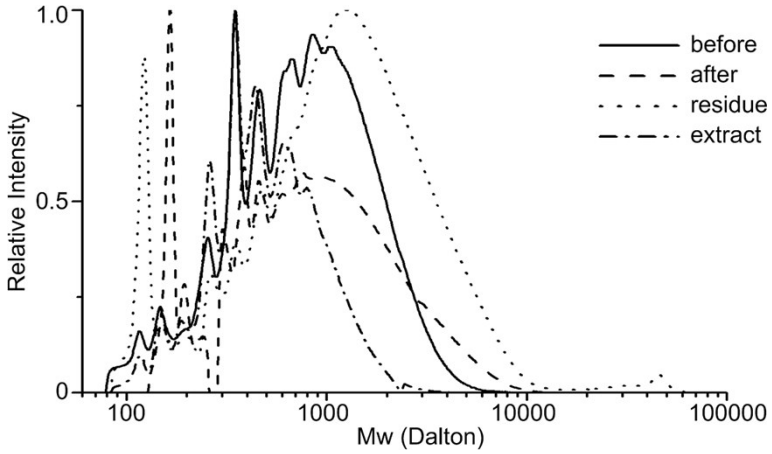

Figure S66. GPC (THF, against polystyrene standards) of different fraction obtained from the depolymerisation of **L23** (15 min, 10 wt% $Fe(OTf)_3$, 30 wt% ethylene glycol, 1,4-dioxane).

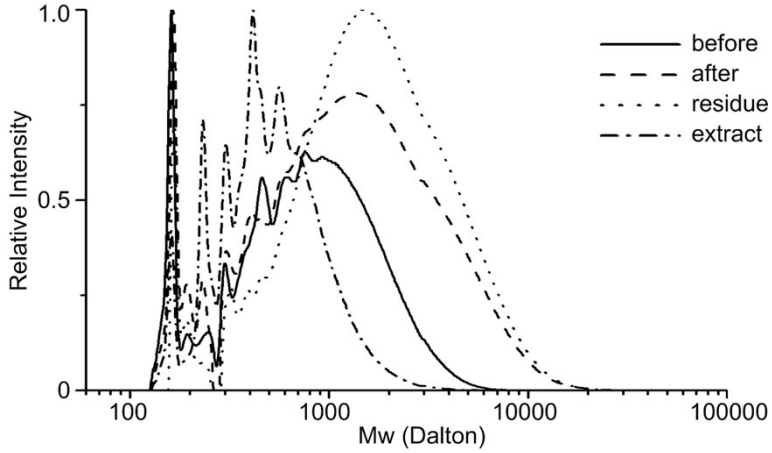

Figure S67. GPC (THF, against polystyrene standards) of different fraction obtained from the depolymerisation of **L24** (15 min, 10 wt% $Fe(OTf)_3$, 30 wt% ethylene glycol, 1,4-dioxane).

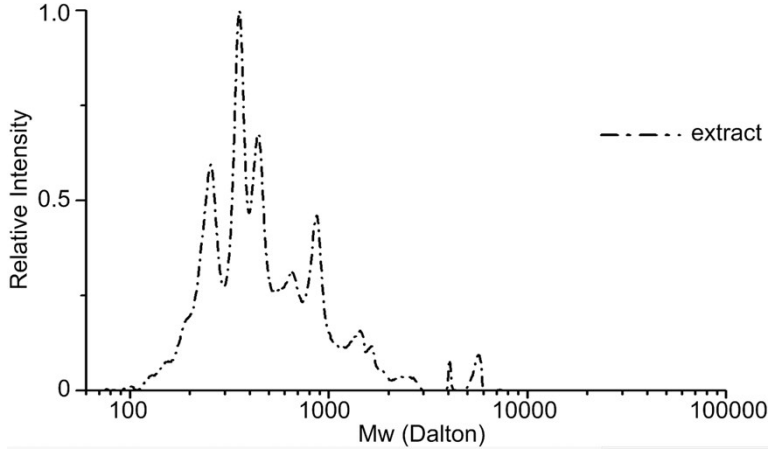

Figure S68. GPC (THF, against polystyrene standards) of the extracted fraction obtained from the depolymerisation of **L25** (15 min, 10 wt% $Fe(OTf)_3$, 30 wt% ethylene glycol, 1,4-dioxane). The other fraction were not soluble in THF and could not be measured.

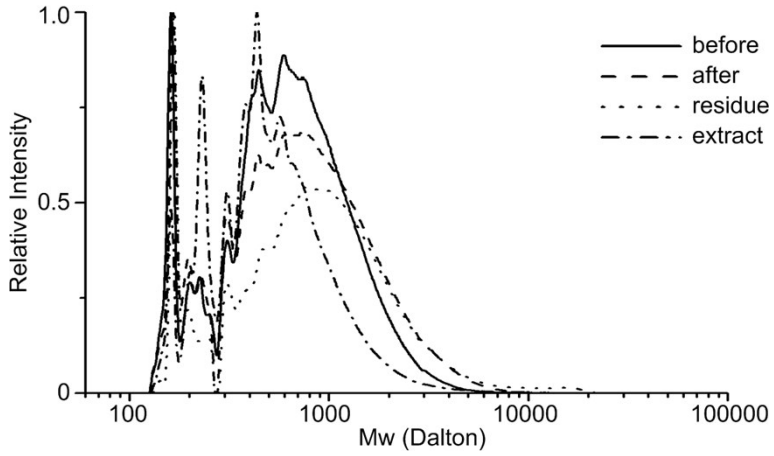

Figure S69. GPC (THF, against polystyrene standards) of different fraction obtained from the depolymerisation of **L26** (15 min, 10 wt% $Fe(OTf)_3$, 30 wt% ethylene glycol, 1,4-dioxane).

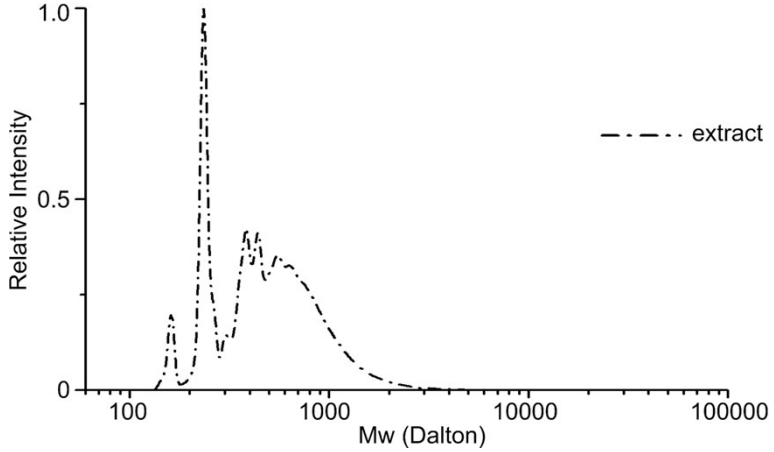

Figure S70. GPC (THF, against polystyrene standards) of the extracted fraction obtained from the depolymerisation of **L27** (15 min, 10 wt% $Fe(OTf)_3$, 30 wt% ethylene glycol, 1,4-dioxane). The other fraction were not soluble in THF and could not be measured.

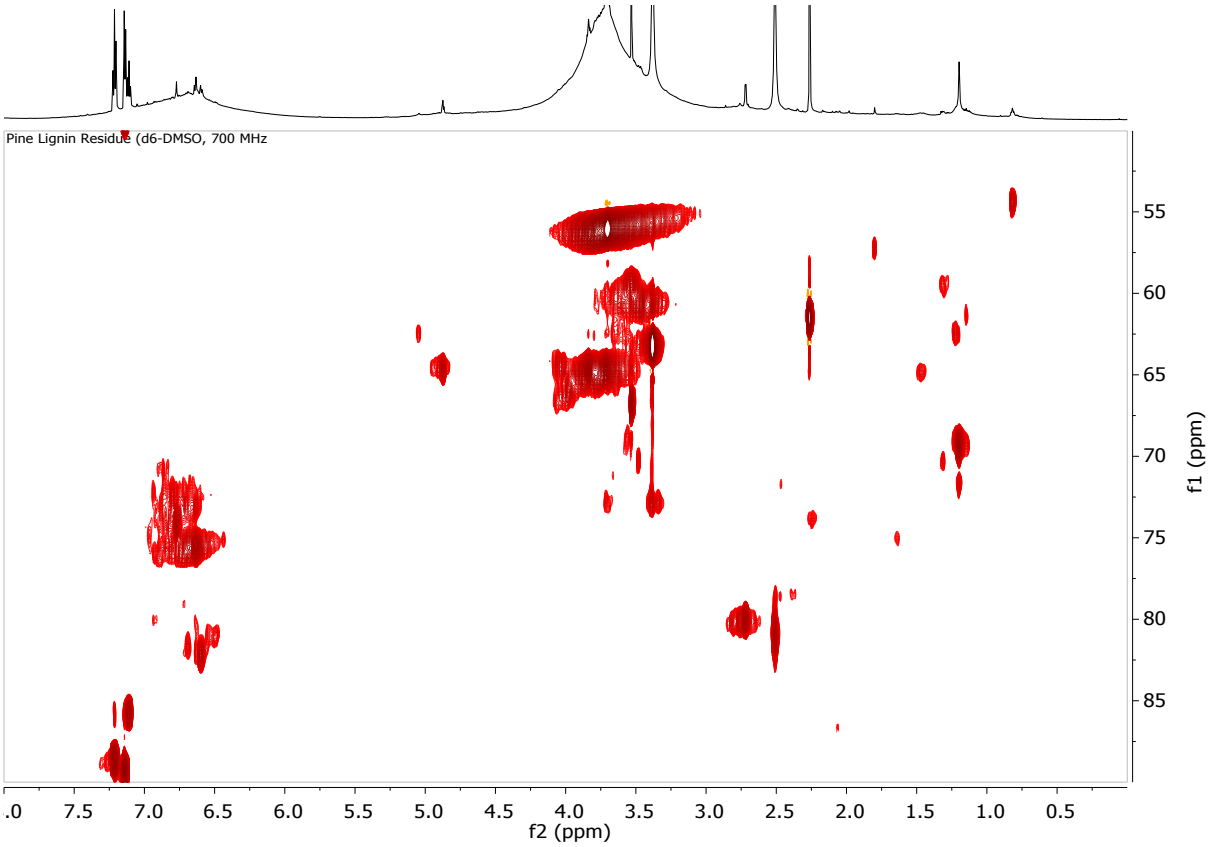

Figure 71. 2D HSQC spectrum of the crude residual obtained after depolymerisation and extraction of low molecular weight material of pine dioxasolv lignin. ^{13}C SW = 50-90ppm

4. Correlation graphs

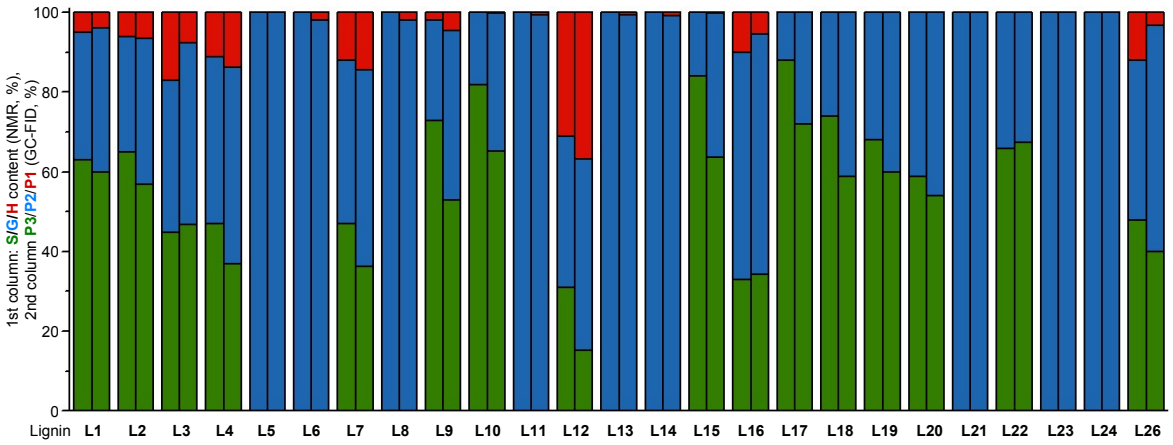

Figure S72. Comparison between first column: S/G/H content (%) and second column **P1**-**3** yields (%).

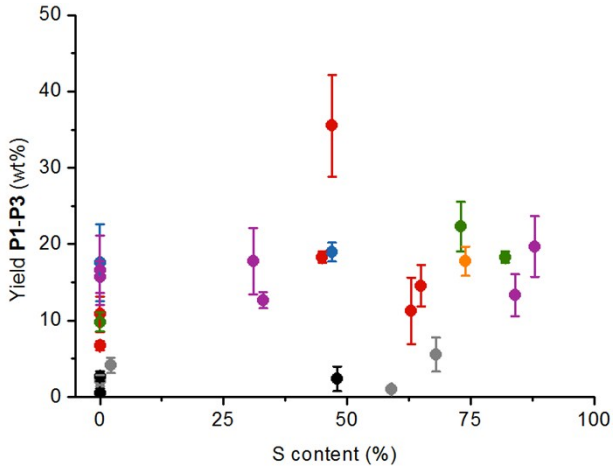

Figure S73: Yield of **P1**-**P3** plotted against the S content of the parent lignin.

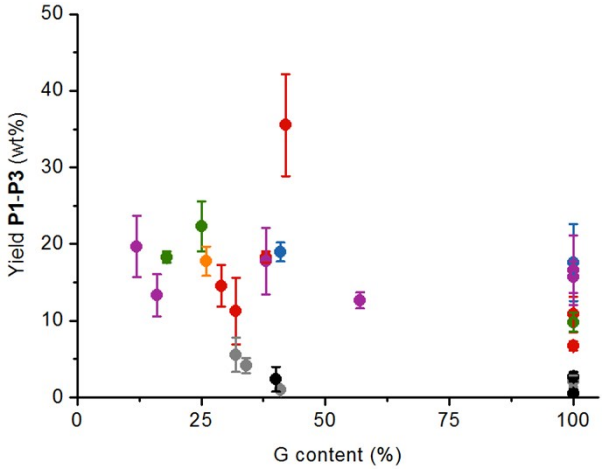

Figure S74: Yield of **P1**-**P3** plotted against the G content of the parent lignin.

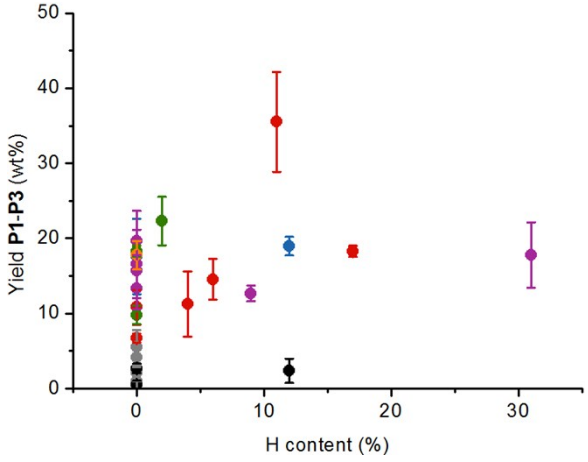

Figure S75: Yield of **P1**-**P3** plotted against the H content of the parent lignin.

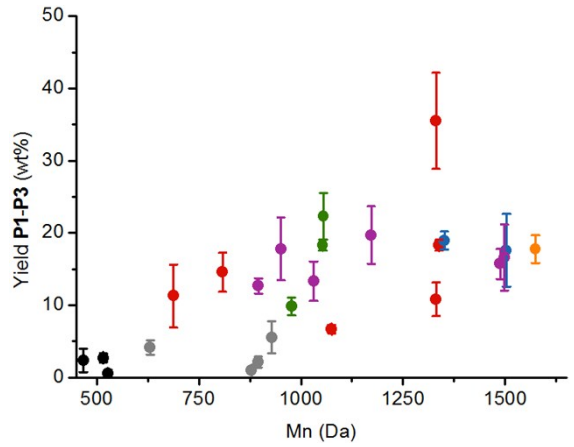

Figure S76: Yield of **P1**-**P3** plotted against the M_n determined by GPC analysis of the parent lignin.

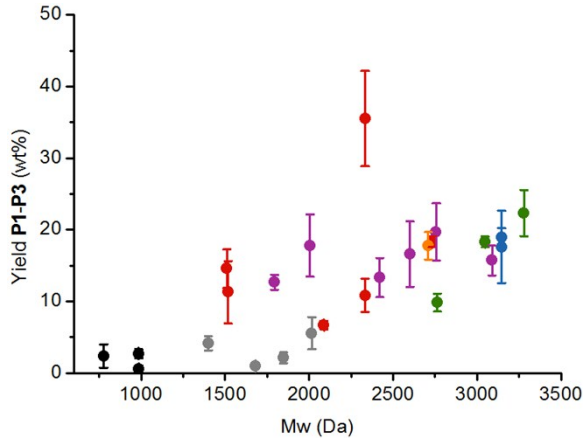

Figure S77: Yield of **P1**-**P3** plotted against the M_w determined by GPC analysis of the parent lignin.

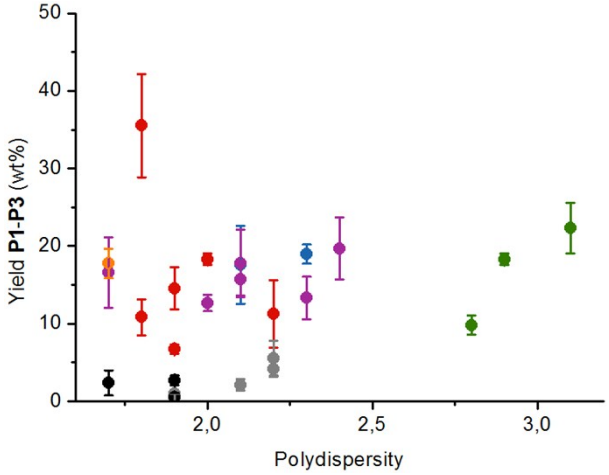

Figure S78: Yield of **P1**-**P3** plotted against the polydispersity (Đ) determined by GPC analysis of the parent lignin.

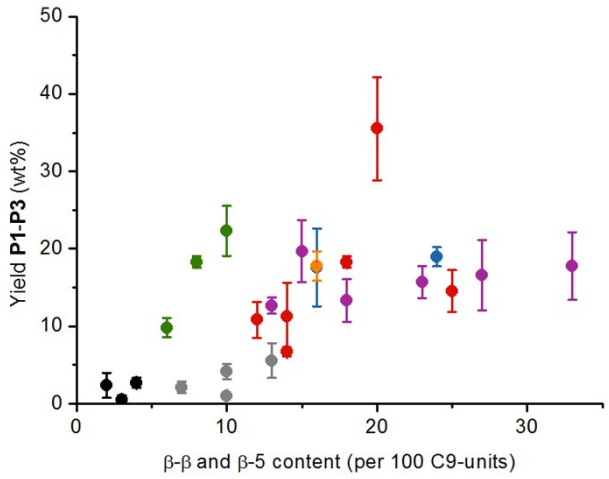

Figure S79: Yield of **P1**-**P3** plotted against the β- β and β-5 content of the parent lignin as determined by 2D HSQC NMR.

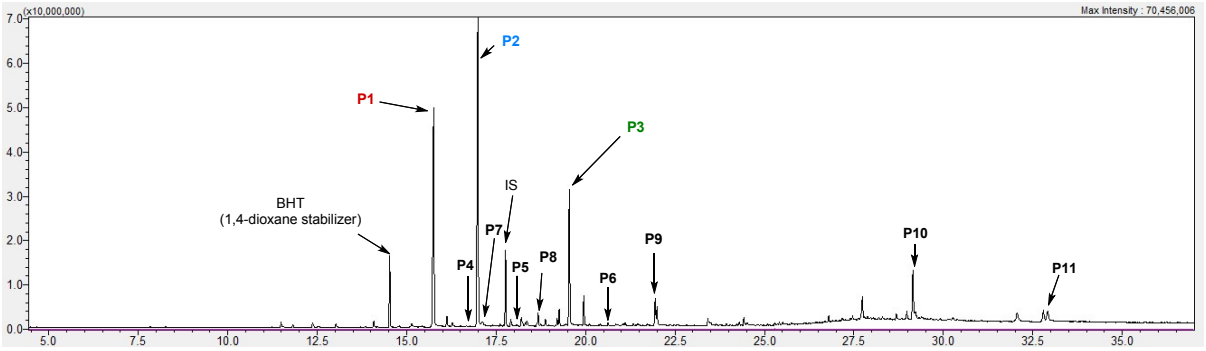

Figure S80. GMCS graph obtained from the low molecular weight fraction from the depolymerisation of **L12**, showing retention times of the identified products discussing the in manuscript.

Table S3. Overview of the quantities of identified products from depolymerisation of **L1**-**L27**.

Lignin	**P1** (wt%)[a]	**P2** (wt%)[a]	**P3** (wt%)[a]	**P4** (wt%)[b]	**P5** (wt%)[b]	**P6** (wt%)[b]	**P7** (wt%)[b]	**P8** (wt%)[b]	**P9** (wt%)[b]	Total **P1**-**P9** (wt%)	**P10** (wt%)[c]	**P11** (wt%)[c]
L1	0.3	3.8	7.2	-	-	0.1	-	trace	0.3	11.7	-	4.4
L2	0.8	5.0	8.8	-	trace	0.1	-	0.1	0.4	15.2	-	3.0
L3	1.1	7.9	9.3	-	trace	0.3	trace	0.1	0.8	19.5	-	1.7
L4	4.0	17.0	14.5	trace	0.4	1.2	0.1	0.5	0.5	38.2	0.1	trace
L5	-	10.8	-	-	0.1	-	-	0.3	-	11.2	1.1	-
L7	2.3	9.1	7.6	-	0.3	0.3	0.1	0.6	0.3	20.3	-	5.7
L8	0.3	16.0	-	-	0.2	-	trace	1.0	-	17.5	2.5	-
L9	0.8	8.9	12.6	-	1.3	1.1	trace	0.5	0.9	26.1	-	2.3
L10	-	5.8	12.5	-	0.6	0.9	-	0.3	0.7	20.8	-	1.9
L11	0.1	9.6	-	-	2.5	-	-	0.3	-	12.5	-	0.1
L12	5.8	8.8	3.2	trace	trace	trace	trace	0.2	0.5	18.5	0.4	1.1
L13	0.1	16.5	-	-	0.3	-	-	0.4	-	17.3	0.3	-
L14	0.1	15.6	-	-	trace	-	-	0.5	-	16.2	0.2	-
L15	-	4.4	8.9	-	trace	0.1	-	0.1	0.6	14.1	-	2.0
L16	0.6	7.3	4.8	-	-	0.2	trace	0.1	2.6	15.6	0.3	0.7
L17	-	5.0	14.7	-	-	-	-	trace	0.5	20.2	-	2.2
L18	-	6.7	11.0	-	0.1	0.2	-	0.2	2.0	20.2	0.2	4.9
L19	-	2.1	3.5	-	-	0.1	-	-	0.3	6.0	-	1.0
L20	-	0.4	0.6	-	trace	trace	-	-	trace	1.0	-	0.3
L21	-	2.0	-	-	0.2	-	-	-	-	2.2	0.4	-
L22	-	1.2	2.9	-	-	-	-	-	-	4.1	-	-
L23	-	0.5	-	-	trace	-	-	-	-	0.5	-	-
L24	-	2.6	-	-	-	-	-	-	-	2.6	-	-
L25	-	0.5	-	-	-	-	-	-	-	0.5	-	-
L26	0.1	1.3	1.0	-	-	-	-	-	-	2.4	-	-
L27	-	0.2	0.3	-	-	-	-	-	-	0.5	-	-

[a] Based on GC-FID calibration against internal standard (n-octadecane)

[b] Using a calculated relative molar response factor[11]

[c] Based on GC-MS calibration against internal standard (n-octadecane)

5. References

[1] P. J. Deuss, C. W. Lahive, C. S. Lancefield, N. J. Westwood, P. C. J. Kamer, K. Barta and J. G. de Vries, *ChemSusChem*, 2016, **9**, 2974.

[2] F. Tran, C. S. Lancefield, P. C. J. Kamer, T. Lebl and N. J. Westwood, *Green Chem.*, 2015, **17**, 244.

[3] W. J. J. Huijgen, G. Telysheva, A. Arshanitsa, R. J. A. Gosselink and P. J. de Wild, *Ind. Crops Prod.*, 2014, **59**, 85.

[4] J. Wildschut, A. T. Smit, J. H. Reith and W. J. J. Huijgen, *Bioresour. Technol.*, 2013, **135**, 58.

[5] P.J. de Wild, R. van der Laan, A. Kloekhorst and E. Heeres, *Environ. Prog. Sustain. Energy*, 2009, **28**, 461.

[6] P. J. Deuss, M. Scott, F. Tran, N. J. Westwood, J. G. de Vries and K. Barta, *J. Am Chem. Soc.*, 2015, **137**, 7456.

[7] C. W. Lahive, P. J. Deuss, C. S. Lancefield, Z. Sun, D. B. Corbes, C. Young, F. Tran, A. M. Z. Slawin, J. G. de Vries, P. C. J. Kamer, N. J. Westwood and K. Barta, *J. Am. Chem. Soc.*, 2016, **138**, 8900.

[8] C. S. Lancefield, I. Panovic, P. J. Deuss, K. Barta and N. J. Westwood, *Green Chem.*, 2017, **19**, 2012.

[9] C. S. Lancefield, O. S. Ojo, F. Tran and N. J. Westwood, *Angew. Chem. Int. Ed.*, 2015, **54**, 258.

[10] J. D. Nguyen, B. S. Matsuura and C. R. J. Stephenson, *J. Am. Chem. Soc*., 2014, **136**, 1218.

[11] J.-Y. de Saint Laumer, E. Cichetti, P. Merle, J. Egger and A. Chaintreau, *Anal. Chem.*, 2010, **82**, 6457.